

PHYTOCHEMICAL CHARACTERIZATION OF *UROCHLOA DISTACHYA* (L.) THROUGH GAS CHROMATOGRAPHY-MASS SPECTROMETRY AND LIQUID CHROMATOGRAPHY-MASS SPECTROMETRY ANALYSIS WITH *IN SILICO* AND *IN VIVO* ANTI-INFLAMMATORY ASSESSMENT IN CARRAGEENAN-INDUCED PAW EDEMA

SMRUTIRANJAN DASH^{1*}, RAJASEKARAN SIDHAN²

¹Department of Pharmacology, Institute of Pharmaceutical Science and Research Center, Bhagwant University, Ajmer, Rajasthan, India.

²Department of Pharmacology, Al-Azhar College of Pharmacy, Thodupuzha, Kerala, India.

*Corresponding author: Smrutiranjana Dash; Email: dash.smruti1992@gmail.com

Received: 23 January 2025, Revised and Accepted: 04 March 2025

ABSTRACT

Objectives: The objective of this study was to evaluate the phytochemical composition and anti-inflammatory activity of chloroform and ethyl acetate extracts of *Urochloa distachya*, alongside *in silico* molecular docking analysis.

Methods: The phytochemical composition of the extracts was analyzed using gas chromatography-mass spectrometry (GC-MS) and liquid chromatography-mass spectrometry (LC-MS) techniques to identify bioactive compounds. The *in vivo* anti-inflammatory activity was assessed using the carrageenan-induced paw edema model in rats, where the reduction in paw edema was measured to evaluate efficacy. In addition, *in silico* molecular docking studies were conducted to determine the binding affinity of identified compounds with key inflammatory targets, including cyclooxygenase-2, 5-lipoxygenase, phosphodiesterase 4, and human peroxiredoxin 5, to explore their potential anti-inflammatory mechanisms.

Results: The GC-MS and LC-MS analyses of chloroform extract of *U. distachya* (CUD) and ethyl acetate extracts of *U. distachya* identified phytoconstituents with notable anti-inflammatory potential. In the carrageenan-induced paw edema model, the CUD demonstrated a significant reduction in paw edema in rats. *In silico* molecular docking revealed that key compounds, including Holothurin acetate, 7,8-Epoxyanostan-11-ol, 3-acetoxy-, and 7,8,12-Tri-O-acetyl-3-desoxy-ingo-3-one, exhibited strong binding affinities with inflammatory targets, ranging from -8.6 to -15.3 kcal/mol.

Conclusion: The chloroform extract of CUD exhibits significant anti-inflammatory activity, supported by both *in vivo* and *in silico* analyses. The identified phytoconstituents demonstrate strong binding affinities with key inflammatory targets.

Keywords: Phytochemicals, Gas chromatography-mass spectrometry, Liquid chromatography-mass spectrometry, Molecular docking, Anti-inflammatory activity, Carrageenan-induced, *Urochloa distachya*, Poaceae.

© 2025 The Authors. Published by Innovare Academic Sciences Pvt Ltd. This is an open access article under the CC BY license (<http://creativecommons.org/licenses/by/4.0/>) DOI: <http://dx.doi.org/10.22159/ajpcr.2025v18i4.53861>. Journal homepage: <https://innovareacademics.in/journals/index.php/ajpcr>

INTRODUCTION

Inflammation is an intricate biological response of tissues to harmful stimuli, including irritants, damaged cells, and bacteria. This protective mechanism is crucial for initiating tissue regeneration and maintaining homeostasis. The method entails the induction of immune cells, the secretion of signaling molecules such as cytokines, and increased blood flow to the damaged region. Acute inflammation is a vital advantageous reaction to injury or infection; conversely, persistent inflammation is linked to various diseases, including aging, cardiovascular disease, cancer, and neurological disorders [1,2]. When the body experiences inflammation, whether from an infection, a mechanical injury, or a burn, its cells begin to build defense mechanisms without external interference [3]. Inflammation is usually divided into two main types, acute inflammation and chronic inflammation [4]. Acute inflammation is an instantaneous, adaptive response characterized by limited specificity, triggered by harmful stimuli such as infection and tissue injury. This advantageous reaction defends against infectious agents, including mycobacterium tuberculosis, protozoa, fungi, and other parasites [5]. The inflammatory response is crucial for providing growth factors and cytokine signals that coordinate the cellular and tissue movements essential for healing. Various studies have revealed that the inflammatory response during standard healing is marked by spatially and temporally variable patterns of different leukocyte subsets [6]. Chronic inflammation is characterized as a sustained, long-term inflammatory response that endures for several months to years. The

magnitude and consequences of chronic inflammation vary depending on the injury's etiology and the body's capacity to mend and surmount the harm [7]. During the inflammatory process, there is a significant production of inflammatory biomarkers, including reactive oxygen species, reactive nitrogen species, tumor necrosis factor- α (TNF- α), interleukin (IL)-1, IL-6, and cyclooxygenase-2 (COX-2). TNF- α , a pro-inflammatory cytokine, serves as a principal regulator of inflammatory cytokine production, influencing inflammation, immunology, cellular homeostasis, and tumor progression [8,9]. Non-steroidal anti-inflammatory drugs (NSAIDs) are mainly used for the management of pain and inflammatory disorders [10]. Examples of NSAIDs used to treat inflammation include aspirin, naproxen, ibuprofen, diclofenac, indomethacin, meloxicam, piroxicam, meclofenamate, mefenamic acid, celecoxib, and etoricoxib. The primary mechanism of action of NSAIDs involves the inhibition of the enzyme cyclooxygenase [11,12]. NSAIDs have been used for the management of inflammation. The escalating side effects, including heart attacks and strokes associated with these therapies, require the substitution of synthetic medications with plant-based alternatives [13]. Table 1 provides an overview of the current drugs used for treating inflammation, highlighting their respective limitations.

Extensive research on plant crude extracts has been undertaken in recent decades, revealing that various plants possess anti-inflammatory activities. Numerous inflammatory disorders can be efficiently managed with phytochemical substances. Alkaloids, flavonoids, polyphenols,

Table 1: Current anti-inflammatory drugs and their limitations

Sl. No.	Name of the drug	Limitation	References
1	Diclofenac	Increased risk of myocardial infarction or stroke	[14]
2	Etodolac	Gastrointestinal complaints	[15]
3	Diflunisal	Contraindicated in patients with thrombocytopenia and chronic kidney disease	[16]
4	Fenoprofen	May causes ulcer	
5	Ibuprofen	Gastrointestinal and cardiovascular complications.	[17]
6	Indomethacin	Most serious side effects such as shortness of breath, swelling, fever, pale skin, nausea, and painful urination.	[18]
7	Ketoprofen	The side effects such as Urticaria, bronchospasm, heartburn, tachycardia, constipation, and pancreatitis.	[19]
8	Meloxicam	Increase the risk of heart attack	[20]
9	Mefenamic acid	Cases of ulcer and bleeding	[21]
10	Nabumetone	The common side effects are nausea, constipation, swelling, headache, and serious side effects such as ulcers, heart attacks, blood clots, and high blood pressure.	[22]
11	Naproxen	If it is taken regularly, it causes stomach ulcers.	[23]
12	Oxaprozin	Gastrointestinal disorders are the most common adverse effects.	[24]
13	Piroxicam	The side effects include abdominal pain, headache, dizziness, diarrhea, peripheral edema, and hypersensitivity reactions.	[25]
14	Sulindac	Not recommended for cardiovascular disorder; it may produce a risk of heart attack, stroke, and blood clots.	[26]
15	Celecoxib	The severe adverse effects include congestive heart failure, liver toxicity, renal toxicity, anaphylactic reactions, and rashes.	[27]

and terpenoids are the primary chemical classes associated with anti-inflammatory, antimicrobial, anticancer, antidiabetic, antimalarial, and neuroprotective properties [28-30]. *Acacia catechu*, *Azadirachta indica*, *Caesalpinia crista*, *Cassia angustifolia*, *Coriandrum sativum*, *Cuscuta reflexa*, *Enicostema littorale*, *Erythrina variegata*, *Euphorbia hirta*, *Euphorbia tirucalli*, *Fagonia cretica*, *Ficus benghalensis*, *Glycyrrhiza glabra*, *Hibiscus rosa-sinensis*, *Nicotiana tabacum*, *Nigella sativa*, and *Tephrosia purpurea* are plants used for their anti-inflammatory properties [31].

Various animal models exist for evaluating anti-inflammatory potency, including carrageenan-induced paw edema, bradykinin-induced paw edema, dextran-induced paw edema, lipopolysaccharide-induced paw edema, histamine-induced paw edema, arachidonic acid-induced ear edema, 5-HT-induced paw edema croton oil/TPA-induced ear edema, oxazolone-induced ear edema, acetic acid, or compound 48/80-induced vascular permeability, and pleurisy model for acute inflammation. Subacute inflammatory models include the granuloma pouch model. The chronic inflammatory model comprises cotton pellet-induced granuloma, formalin-induced paw edema, and complete Freund's adjuvant-induced arthritis [32].

To better understand the chemical diversity and therapeutic potential of plants, phytochemical research is essential for identifying and quantifying bioactive chemicals inside plants. For this objective, several analytical methods have been used, each developed for a particular class of phytochemicals. Because of its great precision and resolution in complex plant matrices, high-performance liquid chromatography (HPLC) finds extensive usage in the separation of non-volatile chemicals, such as flavonoids and phenolics [33]. Gas chromatography-mass spectrometry (GC-MS) offers an effective method for the separation and identification of volatile compounds, including essential oils and alkaloids, due to its sensitivity and specificity [34]. Moreover, ultra-performance liquid chromatography, a sophisticated variant of HPLC, has acquired prominence for its capacity to provide expedited analyses with superior sensitivity and resolution [35]. Fourier transform infrared spectroscopy and nuclear magnetic resonance spectroscopy are essential for identifying functional groups and elucidating the structure of phytochemicals, hence improving the characterization of plant-derived substances [18,36]. With liquid chromatography-mass spectrometry (LC-MS) and ultraviolet-visible spectroscopy, investigators can look into the wide range of chemicals found in plants and find ways to use them in traditional medicine, medicines, and nutraceuticals [37].

Molecular docking is a computer method employed to anticipate the optimal orientation of one molecule when interacting with another molecule, usually a protein, to establish a stable complex. This technique is extensively utilized in pharmaceutical drug discovery and design, as it aids in comprehending molecular interactions at the atomic scale [38,39]. The primary objective of molecular docking is to ascertain the compatibility of a ligand with the binding site of a target protein and to assess the nature and strength of interactions, including hydrogen bonds, hydrophobic interactions, and electrostatic forces, that stabilize the complex [40]. COX-2 is an inducible enzyme that plays a role in the synthesis of pro-inflammatory prostaglandins, and its specific inhibition is a crucial approach to mitigating inflammation [41]. Lipoxygenase (LOX) catalyzes the synthesis of leukotrienes, potent inflammatory mediators, rendering it a significant target in conditions such as arthritis, asthma, and cancer [42]. Phosphodiesterase 4 (PDE4), responsible for the degradation of cyclic AMP, is primarily expressed in immune cells. Its inhibition has shown a reduction in inflammatory cytokine production, positioning it as a promising target for the treatment of conditions such as psoriasis, asthma, and chronic obstructive pulmonary disease [43]. Human peroxiredoxin 5 (HP5) is a crucial antioxidant enzyme that reduces peroxides and protects cells from oxidative stress, a significant factor in the pathophysiology of inflammation-related disorders [44].

Urochloa distachya, commonly known as signal grass, is a perennial grass species belonging to the family Poaceae, it is widespread in tropical and subtropical climates. It grows in grasslands, savannas, and disturbed places, especially in poor soils and degraded soils [45]. Its flexibility has rendered it a beneficial species for preventing soil erosion and enhancing soil structure, especially in regions susceptible to land degradation. Moreover, *U. distachya* is esteemed as a forage crop, providing substantial nutritional benefits for cattle, especially in tropical areas where it functions as a principal feed source during the dry season [46]. Most plants in the Poaceae family are used as traditional treatments to treat diabetes, astringents, ulcers, anthelmintic, hypersensitivity, and inflammation, and as astringents, diuretics, and also used as antioxidant agents [47]. The previous study of GC-MS analysis of methanolic and petroleum ether extract of *U. distachya* revealed the phytoconstituents includes; 7-Methyl-Z-tetradecen-1-ol acetate; 9,12,15-Octadecatrienoic acid, 2,3-dihydroxypropyl ester; (Z, Z, Z); 2-Naphthalenol,2,3,4,4a,5,6,7 octahydro-1,4adimethyl-7-(2-hydroxy-1-methylethyl); 2-[4-methyl-6-(2,6,6-trimethylcyclohex-1-enyl) hexa-1,3,5-trienyl] cyclohex-1-en-1-carboxaldehyde; Spiro[4.5]decan-7-one,1,8-dimethyl-8,9-epoxy-4-isopropyl; 9,12,15-Octadecatrienoic

acid, 2,3-bis[(trimethylsilyl)oxy]propyl ester, (Z, Z, Z); Hexadecanoic acid, methyl ester; phytol; Campesterol; Stigmasterol; Tri-tetracontane; γ -Sitosterol; β -Amyrin; α -Amyrin; 9,19-Cyclolanostane-3,7-diolis which exhibited anti-inflammatory activity [48,49]. Furthermore, the flavonoid and steroid compounds 4H-Pyran-4-one, 2, 3-dihydro-3, 5-dihydroxy-6-methyl, and 26-Nor-5-cholesten-3- α -ol-25-one, identified through GC-MS analysis of the methanolic cold extract of *U. distachya*, are also documented for their anti-inflammatory activity [50].

The present study seeks to comprehensively investigate the phytochemical content and assess the anti-inflammatory properties of chloroform and ethyl acetate extract of *U. distachya* by a combination of GC-MS, LC-MS, *in vivo* anti-inflammatory assays, and molecular docking methods. The carrageenan-induced paw edema model in rats is an established method for testing the anti-inflammatory effectiveness of extracts by measuring paw swelling. Molecular docking analyses can predict the interactions of the identified phytoconstituents with significant inflammatory targets, including COX-2, 5-LOX, PDE4, and HP5.

METHODS

Chemicals and reagents

Collection and preparation of plant

The plant was authenticated by Dr. V. Ranjan (scientist, BSI, Kolkata, India), Voucher number: CNH/Tech.II/2019/77, and the plant samples were collected from the local area of Bargarh district (Hatgaon), Bargarh, Odisha, India. The whole plants were shade-dried, pulverized into powder, and preserved in an air shield container.

Extraction of plant material

The dried, powdered plants were first defatted using petroleum ether to eliminate any waxy residue. Then, the Soxhlet apparatus was used to extract the plants using chloroform and ethyl acetate in the order of their polarity. Finally, a rotary evaporator concentrated the mixture at 40°C. To measure the yield %, the dried extract was stored at 4°C. Using standard protocols, the *U. distachya* extracts were evaluated qualitatively for phytochemicals [51].

Experimental animal care

Twenty-four Wistar albino rats (7–10 weeks old, weighing 155–180 g) were acquired from M/S Chakraborty Enterprises (registration no.: 1443/PO/Bt/s/11/Committee for the Purpose of Control and Supervision of Experiments on Animals [CPCSEA], Kolkata) for anti-inflammatory study and were accommodated in cages. Before the testing, the rats had a 7-day acclimatization period to laboratory conditions, adhering to a 12-h photoperiodic at a temperature of 22±3°C. The animals were provided with conventional pellet diets and unrestricted access to water. Throughout the trial, the cages were sanitized bi-daily and maintained in a hygienic condition to avert infection. The animals received appropriate care under the ethical standards established by the International Guidelines for the Use of Laboratory Animals. The animal tests were conducted in compliance with regulations about the protection of animals utilized in scientific research. Our experiments demonstrated successful anti-inflammatory activity, as evidenced by carrageenan-induced paw edema. This validated our utilization of rats in a carrageenan-induced paw edema model to find out the anti-inflammatory effect of *U. distachya*.

Ethical statement

All experiments were conducted in complete adherence to international norms. The design protocol received approval from the Animal Ethical Committee (1376/PO/Re/S/10/CPCSEA) under project proposal numbers IAEC/01/2024 for the acute toxicity study and IAEC/03/2024 for carrageenan-induced paw edema in rats.

GC-MS analysis

GC-MS analysis was conducted with Agilent 5977 MSD technology. The mass spectrophotometer features an HP-5 MS fused silica column

of 30 m×250 μ m×0.25 μ m. It is linked to an MSD interface. Helium served as the carrier gas, and the column flow rate was established at 1.2 ml/min. The temperature of the column varied from 60°C to 325°C (350°C), with a pressure of 11.367 psi. The whole duration of the GC operation was 40 min. A volume of 1 μ L of the sample was pushed, and the mass was determined at an energy level of 70 electron volts. The quad temperature was established at 150°C, but the source temperature was configured to 230°C for a maximum length of 10 min. The chromatogram displayed the concentration of the chemical in the chloroform extract of *U. distachya* (CUD) and ethyl acetate extracts of *U. distachya* (EAUD) as a percentage [48].

LC-MS analysis

LC-MS (Agilent Technologies, USA), Direct Infusion Mass with ESI and APCI (Positive and Negative ion mode), 1260 Infinity Nano HPLC with Chipcube, and 6550 iFunnel Q-TOFs. A source temperature of 140°C was maintained for the full-scan mode (m/z 100–1200). A solvent mixture of 0.3% formic acid in methanol and a C-8 column (Phenomenex, 5 μ , 2 mm, id) were used to analyze the compounds, with a flow rate of 0.1 mL/min. All gas parameters were kept constant during the test: 6 ml/min gas flow, 25 psi nebulizing pressure, and 350°C drying gas temperature. Centrifuged at 12,000 rpm for 10 min, the CUS and EAUD extracts (0.5 g) were diluted in methanol before analysis. To determine the mass fragmentation of the compounds, the Spectrum Database for Organic Compounds (SDBS) was used [52].

Acute toxicity study

In line with the Organization for Economic Cooperation and Development (OECD) guideline 423 (Annexure 2b), an acute oral toxicity study took place [53]. Three rats from each group, CUD and EAUD, were randomly selected at a dosage of 2000 mg/kg body weight. The samples were solubilized in a solution of 1% carboxymethylcellulose (CMC) and 3% dimethyl sulfoxide. Post-treatment, the rats were monitored for any behavioral alterations during the initial 4 h, followed by an additional 48 h of inspection. The rats were monitored daily for 14 days. This study aimed to ascertain the emergence of clinical or toxicological symptoms as per the guidelines set by the OECD. All observations, including alterations in the skin, eyes, and mucous membranes, alongside behavioral patterns such as food consumption, body weight, temperature, respiration, lethargy, sedation, unconsciousness, and mortality, were meticulously documented and maintained in a distinct record. No signs of toxicity or mortality were observed after 14 days. Doses of 400 mg/kg for CUD and EAUD showed the most significant safety for anti-inflammatory activity.

Evaluation of anti-inflammatory activity

The rats were categorized into four groups, each comprising six rats. Paw edema was induced by administering 0.1 mL of 1% w/v carrageenan dissolved in 1% CMC and injected into the sub-plantar tissues of the left hind paw of each rat [54].

- Group I (Carrageenan control): 0.1 mL of 1% w/v carrageenan
- Group II (Positive control): Indomethacin 10 mg/kg b.w. + 0.1 mL of 1% w/v carrageenan
- Group III (Test I): CUD 400 mg/kg b.w. + 0.1 mL of 1% w/v carrageenan
- Group IV (Test II): EAUD 400 mg/kg b.w. + 0.1 mL of 1% w/v carrageenan.

The paw's thickness was measured using a Vernier Caliper just before and after the injection of carrageenan at 60, 120, 180, and 240 min. The percentage inhibition of edema in the test group compared to the carrageenan control group was used to calculate the anti-inflammatory activity.

The percentage inhibition of edema is calculated using the formula:

$$\% \text{ inhibition} = \frac{T_0 - T_t}{T_0} \times 100$$

Where T_t is the thickness of the paw of the test group, and T_o is the paw thickness of the control group.

Molecular docking analysis

Molecular docking was performed using the phyto-constituents identified from GC-MS analysis of CUD and EAUD. The 3D structures of COX-2 (PDB ID: 3 mdl) [55], 5-LOX (PDB ID: 6 ncf) [56], PDE4 (PDB ID: 4 wcu) [57], and HP5 (PDB ID: 1 hd2) [58] were obtained from the Protein Data Bank. The 3D structure of Triamcinolone Acetonide (PubChem CID 6436), Campesterol (PubChem CID 173183), Docosanoic acid, 1,2,3-propanetriyl ester (PubChem CID 62726), 7,8-Epoxy lanostan-11-ol, 3-acetoxy- (PubChem CID 541562), Anodendroside E 2 (PubChem CID 91692722), 7,8,12-Tri-O-acetyl-3-desoxy-ingol-3-one (PubChem CID 541413), 9-Octadecenoic acid (Z)-, 3-[(1-oxohexadecyl) oxy]-2-[(1-oxooctadecyl) oxy] propyl ester (PubChem CID 5365005), Epoxycholesterol (PubChem CID 227037), Holothurin acetate (PubChem CID 541418), Octadecanoic acid, 1-[(1-oxohexadecyl) oxy] methyl]-1,2-ethanediyl ester (PubChem CID 91865316), Fluprednisolone (PubChem CID 5876), (\pm)9-HpODE (PubChem CID 6439847), (\pm)12(13)-DiHOME (PubChem CID 10236635), 2-(4-Amino-1,2,5-oxadiazol-3-yl)-1-ethyl-N-[2-(methylamino) ethyl]-1H-imidazo[4,5-c] pyridine-7-carboxamide (PubChem CID 25023715), 2,2-Dimethyl-4-[(octadecyloxy)methyl]-1,3-dioxolane (PubChem CID 568294), 2-Hydroxy-2-octyldecanedioic acid (PubChem CID 622473), 2-Nitro-4-nonanol (PubChem CID 544004), 3-(4-Methylphenyl) glutamic acid (GLU) (PubChem CID 319713), 3,4-Dihydro-2H-1,6-benzoxazocin-5(6H)-one (PubChem CID 550286), 6-Gingerol (PubChem CID 442793), Dihydro-1H,5H-dipyrrolo[1,2-a:1'2'-d] pyrazine-2,5,7,10 (3H,8H,10aH)-tetrone (PubChem CID 544479), Ethepon (PubChem CID 27982), Ethyl 2-phenylethyl butylphosphonate (PubChem CID 6421933), Maltol (PubChem CID 8369), Methyl 3-[4-(2-methoxy-2-oxoethyl)-4-methyl-2,5-dioxo-3-pyrrolidinyl] propanoate (PubChem CID 597324), N-Benzylformamide (PubChem CID 80654), Phosphoglycolate (PubChem CID 529), TMB-8 (PubChem CID 5494), Traumatic Acid (PubChem CID 5283028), 2-Aminoadipic acid (PubChem CID 469), 2-Cyclohexyl-2-hydroxyacetamide (PubChem CID 236593), 4-Undecylbenzenesulfonic acid (PubChem CID 38222), 9-Oxo-10(E),12(E)-octadecadienoic acid (PubChem CID 5283011), Methyl 12-hydroxystearate (PubChem CID 8840), NP-008993 (PubChem CID 53851542), Oleamide (PubChem CID 5283387), Pyrogallol (PubChem CID 1057) were taken from PubChem. The proteins were designed with AutoDock tools-1.5.7, and the docking operation was carried out using the crystallographic structure chain A [59]. To determine the active site, the water molecules and co-crystal ligands were removed, followed by the addition of polar hydrogen, and then the Kollman charge was applied. The ligands were made using the Open Babel software (v.2.4.1) [60]. Active regions were found to be the parts of the amino acids that bind with the ligands shown in the protein files. To cover these areas, a grid box was made. For COX-2, 5-LOX, and PDE4, the grid box was set to have 60×60×60 x, y, and z points. For HP-5, it was set to 40×40×40. For COX-2, the grid center was set at 25.924, 21.223, and 65.974; for 5-LOX, it was 24.889, -22.451, and 33.681; for PDE4, it was 19.048, -11.068, and -4.778; and for HP-5, it was 8.009, 42.610, and 20.044. The docking score was determined using the AutoDock Vina software, and the 3D visualization was done using the Biovia Discovery Studio 2021 Client [61].

Statistical analysis

The statistical data were analyzed using a one-way analysis of variance followed by *post hoc* Tukey honestly significant difference test (Statistical Package for the Social Sciences v. 21, IBM corporation and MS EXCEL v. 2019), with value as mean±standard error mean. “p”<0.05 were considered statistically significant.

RESULTS

GC-MS analysis of chloroform and ethyl acetate of *U. distachya*

The GC-MS chromatograms of CUD and EAUD are illustrated in Fig. 1 and Table 2, representing the compounds' retention time, name of the compounds, nature of the compounds, molecular formula, molecular

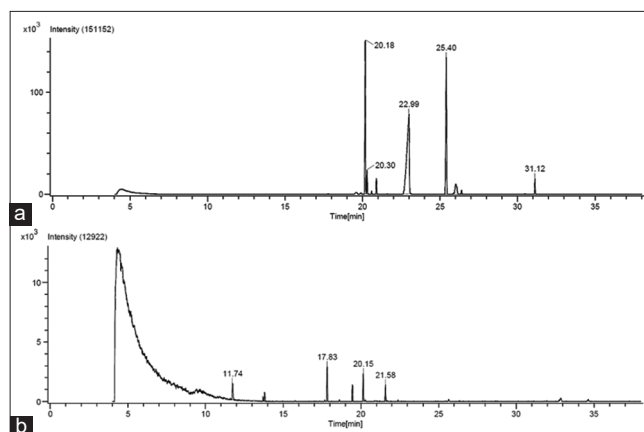


Fig. 1: Gas chromatography-mass spectrometry chromatogram of (a) chloroform, and (b) ethyl extract of *Urochloa distachya*

weight, peak area percentage, and biological activity. The structures of the phyto-compounds are illustrated in Fig. 2. The CUD possessed nine phytoconstituents, β Carotene (21.66); Triamcinolone Acetonide (2.97); Campesterol (1.83); Docisanoic Acid, 1,2,3-Propanetriyl ester (42.09); 7,8-Epoxy lanostan-11-ol,3-acetoxy-(24.13); Anodendroside E 2 (0.24); Cholestan-3-ol,5-Chloro-6-Nitro-, (3 β , 5 α , 6 β)-(4.62); 7,8,12-Tri-O-Desoxy-ingol-3-one(0.63); 9-Octadecenoic Acid(Z)-, 3-[(1-Oxohexadecyl) Oxy]-2-[(1-Oxooctadecyl) Oxy] Propyl Ester (1.84). EAUD were revealed seven phytoconstituent, Epoxycholesterol (15.56); 9-Octadecenoic acid (Z)-, 3-[(1-oxohexadecyl)oxy]-2-[(1-oxooctadecyl)oxy] propyl ester (3.39); Holothurin acetate (7.85); Octadecanoic acid, 1-[(1-oxohexadecyl)oxy]methyl]-1, 2-ethanediyl ester (26.08); Fluprednisolone (12.73); 7,8-Epoxy lanosta-11-ol, 3-acetoxy-(21.15); Cholestan-3-ol, 5-chloro-6-nitro-, (3 β , 5 α , 6 β)-(13.25).

LC-MS analysis of chloroform and ethyl acetate of *U. distachya*

The LC-MS/MS chromatograms of CUD and EAUD are illustrated in Figs. 3 and 5, and the structure of the compounds is depicted in Figs 4 and 6. Tables 3 and 4 represent the peak number, retention time, identified compounds, ion, molecular formula, molecular weight, and biological activity. The positive ion mode ($M+H$)⁺ of the CUD indicated the probable compounds as such; Maltol; 2-Nitro-4-Nonanol; 3,4-Dihydro-2H-1,6-Benzoxazocin-5(6H)-One; N-Benzylformamide; Methyl 3-[4-(2-Methoxy-2-Oxoethyl)-4-Methyl-2,5-Dioxo-3-Pyrrolidinyl] Propanoate; 2-(4-Amino-1,2,5-oxadiazol-3-yl)-1-ethyl-N-[2-(methylamino) ethyl]-1H-imidazo[4,5-c]pyridine-7-carboxamide; (3Z)-3-[4-[2-(4-Methoxyphenyl)-2-oxoethoxy] benzylidene]-6-methyl-2,3-dihydro-4H-thiochromen-4-one; 6-Gingerol; (\pm) 12(13)-DiHOME; TMB-8; 1,3-Diacetoxy-7,8-dimethyl-7-[(2E)-3-methyl-2,4-pentadiene-1-yl]-3,5,6,6a,7,8,9,10-octahydronaphtho[1,8a-c] furan-5-yl-4-hydroxybenzoate; Ethephon; Methylamine; Hexyl 2-propylheptyl phthalate; Ethepon; Phosphoglycolate. Negative ion mode [$M-H$]⁻ identified the compounds in *U. distachya* chloroform extract; D-(-)- Mannitol; 3-(4-Methylphenyl) GLU; Dihydro-1H,5H-dipyrrolo[1,2-a:1'2'-d]pyrazine-2,5,7,10(3H,8H,10aH)-tetrone; NP-014937; Traumatic Acid; 2-Hydroxy-2-octyldecanedioic acid; Ethyl 2-phenylethyl butylphosphonate; (\pm) 9-HpODE; Tetradecyl N-(ethoxycarbonyl)alaninate; Glycol stearate; 2,2-Dimethyl-4-[(octadecyloxy)methyl]-1,3-dioxolane. The positive ion mode ($M+H$)⁺ of the ethyl acetate extract of *U. distachya* showed compounds such as; 2,4,5,6-Tetrachloro nicotinamide; 2-Acetamido-1,5-anhydro-2-deoxyhex-1-enitol; 2-Cyclohexyl-2-hydroxyacetamide; Pyrogallol; 1-Allyl-2-benzyl-1,2-dihydropyridine; (4R,4bR,8S,10aR,10bR,12aS)-8-Hydroxy-10a,12a-dimethyl-3,4,4a,4b,5,7,8,9,10,10a,10b,11,12,12a-tetradecahydronaphtho[2,1-f]quinolin-2(1H)-one; 4-[5-Acetoxy-8,8-dimethyl-6-(3-methyl-2-buten-1-yl)-4-oxo-4H,8H-pyrano[2,3-f]chromen-3-yl]-1,2-phenylene diacetate; NP-008993; Oleamide; 9-Oxo-10(E),12(E)-octadecadienoic acid; 2-Methoxy-

Table 2: GC-MS study of CUD and EAUD

Sl. No.	Rt (min)	Name of the compound	Nature	M.F.	M.W.	Peak area %	Biological activity	References
01	20.18	β Carotene	Polyunsaturated hydrocarbon	$C_{40}H_{56}$	536.9	21.66	Antibacterial, Antioxidant, and Antidiabetic activity.	[62,63]
02	20.30	Triamcinolone Acetonide	Corticosteroid	$C_{24}H_{31}FO_6$	434	2.97	Anti-inflammatory, analgesic, rheumatoid arthritis, Addison's disease, leukemia, osteoarthritis, and hypersensitivity. Spasticity. Itching, redness, inflammation, severe allergic reactions, severe colitis, tendons, lung disorders, blood cell disorders, inflammation, and eye disorders.	[64-66]
03	20.90	Campesterol	Steroidal compound	$C_{28}H_{48}O$	400	1.83	Anti-inflammatory and cytotoxic activity. Antioxidant and anticancer. Antibacterial.	[48,67,68]
04	22.99	Docosanoic acid, 1,2,3-propanetriyl ester	Fatty acid ester	$C_{69}H_{134}O_6$	1058	42.09	Emulsifying agent, skin conditioning agent, and surfactant. Antioxidant, nematocide, and hypocholesterolemic activity.	[69,70]
05	25.40	7,8-Epoxy lanostan-11-ol, 3-acetoxy-	Alcoholic	$C_{32}H_{54}O_4$	502	24.13	Anti-inflammatory, antimicrobial activity.	[71,72]
06	25.86	Anodendroside E 2	NA	$C_{30}H_{38}O_{11}$	574	0.24	Antimicrobial.	[73]
07	26.02	Cholestan-3-ol, 5-Chloro-6-Nitro-, (3 beta, 5 alpha, 6 beta) -	NA	$C_{27}H_{46}ClNO_3$	468.1	4.62	Not Reported	
08	26.39	7,8,12-Tri-O-acetyl-3-desoxy-ingol-3-one	NA	$C_{26}H_{34}O_9$	490	0.63	Antioxidant and antibacterial activity.	[74]
09	31.12	9-Octadecenoic acid	NA	$C_{55}H_{104}O_6$	860	1.84	Emulsifying agent.	[75]
		(Z)-, 3-[[[1-oxohexadecyl] oxy]-2-[[1-oxooctadecyl] oxy] propyl ester						
10	11.74	Epoxycholesterol	Steroid	$C_{27}H_{46}O_2$	402.7	15.56	Decreases ABCA1 and ABCG1-mediated cholesterol efflux.	[76,77]
11	13.70	9-Octadecenoic acid (Z)-, 3-[[[1-oxohexadecyl] oxy]-2-[[1-oxooctadecyl] oxy] propyl ester	Long chain fatty acid	$C_{55}H_{104}O_6$	860	3.39	Marked pro-inflammatory and cytotoxic effects. Emulsifying.	[75]
12	13.80	Holothurin acetate	Triterpene glycoside	$C_{33}H_{48}O_7$	556	7.85	Antischistosomal agent.	[78]
13	17.83	Octadecanoic acid, 1-[[[1-oxohexadecyl] oxy] methyl]-1,2-ethanediylolester	Long-chain fatty acid	$C_{55}H_{106}O_6$	863.4	26.08	Drug synthesis-Osteosarcoma.	[79]
14	19.45	Fluprednisolone	Fluorinated Steroid	$C_{21}H_{27}FO_5$	378	12.73	Anti-inflammatory activity.	[80]
15	20.15	7,8-Epoxy lanostan-11-ol, 3-acetoxy-	Alcoholic compound	$C_{32}H_{54}O_4$	502	21.15	Anti-inflammatory and antimicrobial activity.	[81,82]
16	21.58	Cholestan-3-ol, 5-Chloro-6-Nitro-, (3 beta, 5 alpha, 6 beta)-	NA	$C_{27}H_{46}ClNO_3$	468.1	13.25	Not Reported	

GC-MS: Gas chromatography-mass spectrometry, CUD: chloroform extract of *Urochloa distachya*, EAUD: Ethyl acetate extracts of *Urochloa distachya*

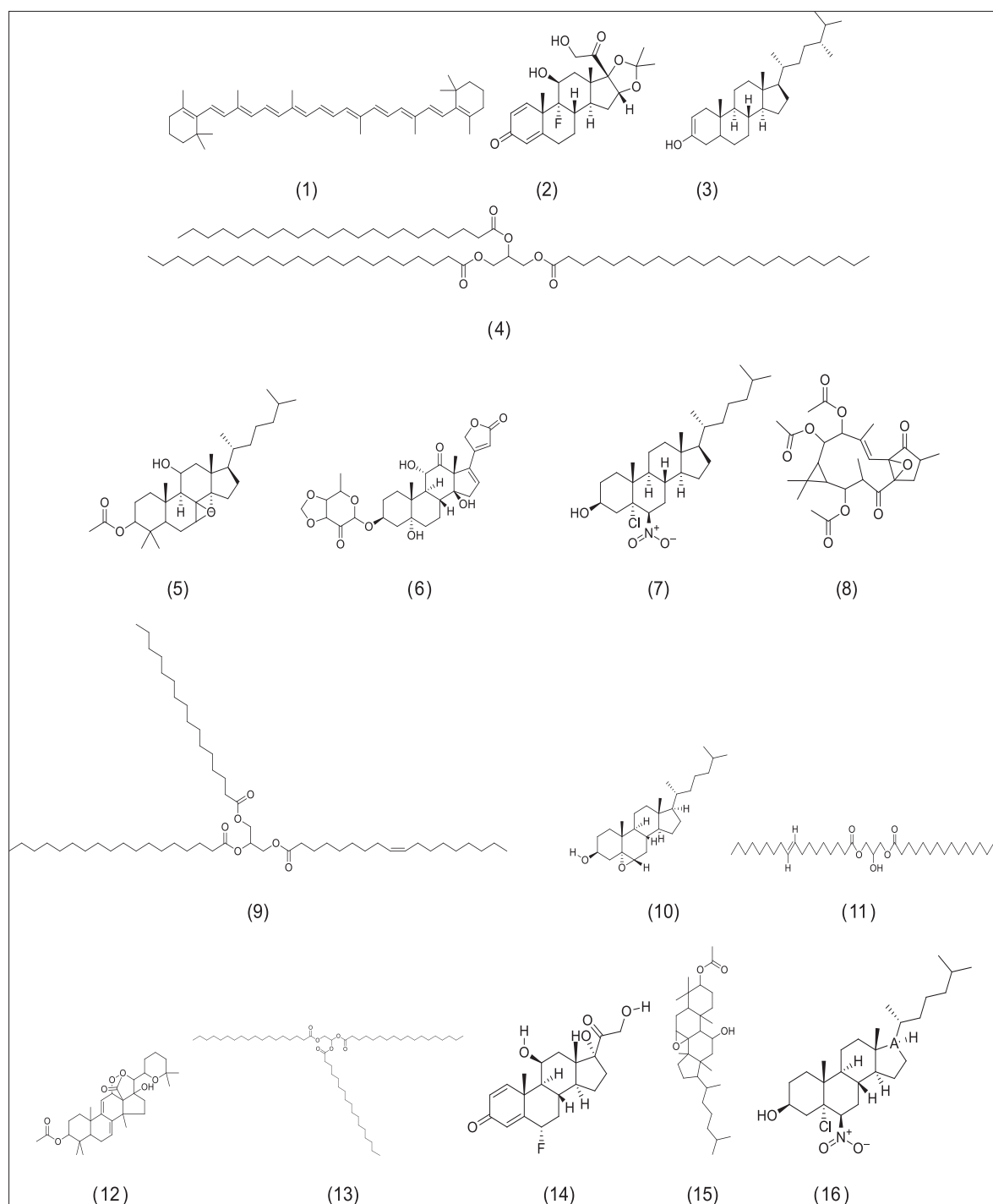


Fig. 2: Structure of the compounds from gas chromatography-mass spectrometry analysis of chloroform and ethyl acetate extract of *Urochloa distachya*

N,N-diundecylacetamide; 2-Aminoadipic acid; Hexyl2-propylheptyl phthalate; N,N'-ethylenebis palmitamide; N-2-Propyn-1-ylcysteine. Negative ion mode (M-H)⁻ found the compounds in the ethyl acetate extract of *U. distachya* were; D-(-)-Mannitol; 3-hydroxy-2-[[[(2E)-3-(4-hydroxyphenyl)prop-2-enoyl]oxy]-3-(methoxycarbonyl) pentanedioic acid; 4-Undecylbenzenesulfonic acid; Tetradecyl N-(ethoxycarbonyl) alaninate; Glycol stearate; Methyl 12-hydroxystearate; NP-021293.

Anti-inflammatory activity

Table 5 and Fig. 7 represent the graph of change in paw edema. Fig. 8 compares the effects of CUD and EAUD extracts and the conventional

drug on the carrageenan control during different intervals in a carrageenan-induced paw edema model using a Vernier Caliper. Administration of CUD at a dosage of 400 mg/kg body weight orally inhibited carrageenan-induced paw edema, exhibiting percentage inhibitions of 22.89%, 31.80%, 57.89%, and 57.9% at 1-4 h. Similarly, the administration of EAUD exhibited percentage inhibitions of 5.38%, 5.64%, 31.73%, and 26.5%, respectively. Indomethacin administered at 10 mg/kg orally inhibited carrageenan-induced paw edema by 43.09%, 50.32%, 75.15%, and 83.7% at 1, 2, 3, and 4 h, respectively.

Table 3: LC-MS analysis of positive (M+H)⁺ and negative (M-H)⁻ ion mode of CUD

Sl. No.	Name of the compound	Nature	M.F.	M.W.	Biological activity	References
1	Maltol	Organic compound	C ₆ H ₆ O ₃	126.03	Antimicrobial activity, natural preservative for cosmetic formulation.	[83,84]
2	2-Nitro-4-nonanol	-	C ₈ H ₁₉ N O ₃	189.14	Not reported	
3	3,4-Dihydro-2H-1,6-benzoxazocin-5 (6H)-one	Benzoxazine	C ₁₀ H ₁₁ N O ₂	177.08	Not reported	
4	N-Benzylformamide	Aromatic compound	C ₈ H ₉ NO	135.06	Not reported	
5	Methyl 3-[4-(2-methoxy-2-oxoethyl)-4-methyl-2,5-dioxo-3-pyrrolidinyl] propanoate	-	C ₁₂ H ₁₇ N O ₆	271.10	Not reported	
6	2-(4-Amino-1,2,5-oxadiazol-3-yl)-1-ethyl-N-[2-(methylamino) ethyl]-1H imidazol[4,5-c] pyridine-7-carboxamide	-	C ₁₄ H ₁₈ N ₈ O ₂	330.16	Not reported	
7	(3Z)-3-[4-[2-(4-Methoxyphenyl)-2-oxoethoxy] benzylidene]-6-methyl-2,3-dihydro-4H-thiophen-4-one	-	C ₂₆ H ₂₂ O ₄ S	430.12	Not reported	
8	6-Gingerol	Phenolic	C ₁₇ H ₂₆ O ₄	294.18	Anticancer, anti-inflammatory, antioxidant activity.	[85]
9	(±) 12 (13)-DIHOME					
10	TMB-8					
11	1,3-Diacetoxy-7,8-Dimethyl-7-[(2E)-3-Methyl-2,4-Pentadien-1-yl]-3,5,6,6a, 7,8,9,10-Octahydronaphtho[1,8a-c] Furan-5-yl/4-Hydroxybenzoate	Trihydroxybenzoic acid	C ₁₈ H ₁₆ O ₄ C ₂₂ H ₂₃ N O ₅ C ₃₁ H ₃₈ O ₈	314.24 395.27 538.26	Ca2+antagonist Not reported	[86]
12	Dilauryl Methylamine	-	C ₂₅ H ₅₃ N	367.42	Not reported	
13	Hexyl 2-propylheptyl phthalate	Organic compound	C ₃₀ H ₅₈ O ₄	390.28	Not reported	
14	Ethephon	Phosphonic acid	C ₂ H ₆ Cl O ₃ P	143.97	Fruit and vegetable ripener	[87]
15	Phosphoglycolate	Monocarboxylic acid	C ₂ H ₅ O ₆ P	155.98	Not reported	
16	D-(-)-Mannitol	Sugar alcohol	C ₆ H ₄ N ₂ OP ₂	181.98	Cerebral edema, decreased intra-ocular pressure, diuresis, reduced renal cell swelling.	[88]
17	3-(4-Methylphenyl) glutamic acid	Amino acid	C ₁₂ H ₁₅ NO ₄	237.10	Not reported	
18	Dihydro-1H,5H-dipyrrolo[1,2-a:1',2'-d] pyrazine-2,5,7,10 (3H,8H,10aH)-tetrone	-	C ₁₀ H ₁₀ N ₂ O ₄	222.06	Not reported	
19	NP-014937	-	C ₂₅ H ₂₆ O ₁₃	534.14	Not reported	
20	Traumatic Acid	Monounsaturated ted straight-chain dicarboxylic acid, Plant hormone	C ₁₂ H ₂₀ O ₄	228.14	Antioxidant activity, arterial hypertension, skin diseases.	[89]
21	2-Hydroxy-2-octyldecanedioic acid	Hydroxy fatty acid	C ₁₈ H ₃₄ O ₅	330.24	Note reported	
22	Ethyl 2-phenylethyl butylphosphonate	Phosphonic ester	C ₁₄ H ₂₃ O ₃ P	270.14	Not reported	
23	(±) 9-HpODE	Hydroperoxy polyunsaturated fatty acid	C ₁₈ H ₃₂ O ₄	312.23	Antimicrobial activity	[90]
24	Tetradecyl N-(ethoxycarbonyl) alaninate	-	C ₂₀ H ₃₉ NO ₄	357.29	Not reported	
25	Glycol stearate	Organic compound	C ₂₀ H ₄₀ O ₃	328.30	Emulsifying agent.	[91]
26	2,2-Dimethyl-4-[(octadecyloxy) methyl]-1,3-dioxolane	-	C ₂₄ H ₄₈ O ₃	384.36	Not reported	

LC-MS: Liquid chromatography-mass spectrometry, CUD: chloroform extract of *Urochloa distachya*

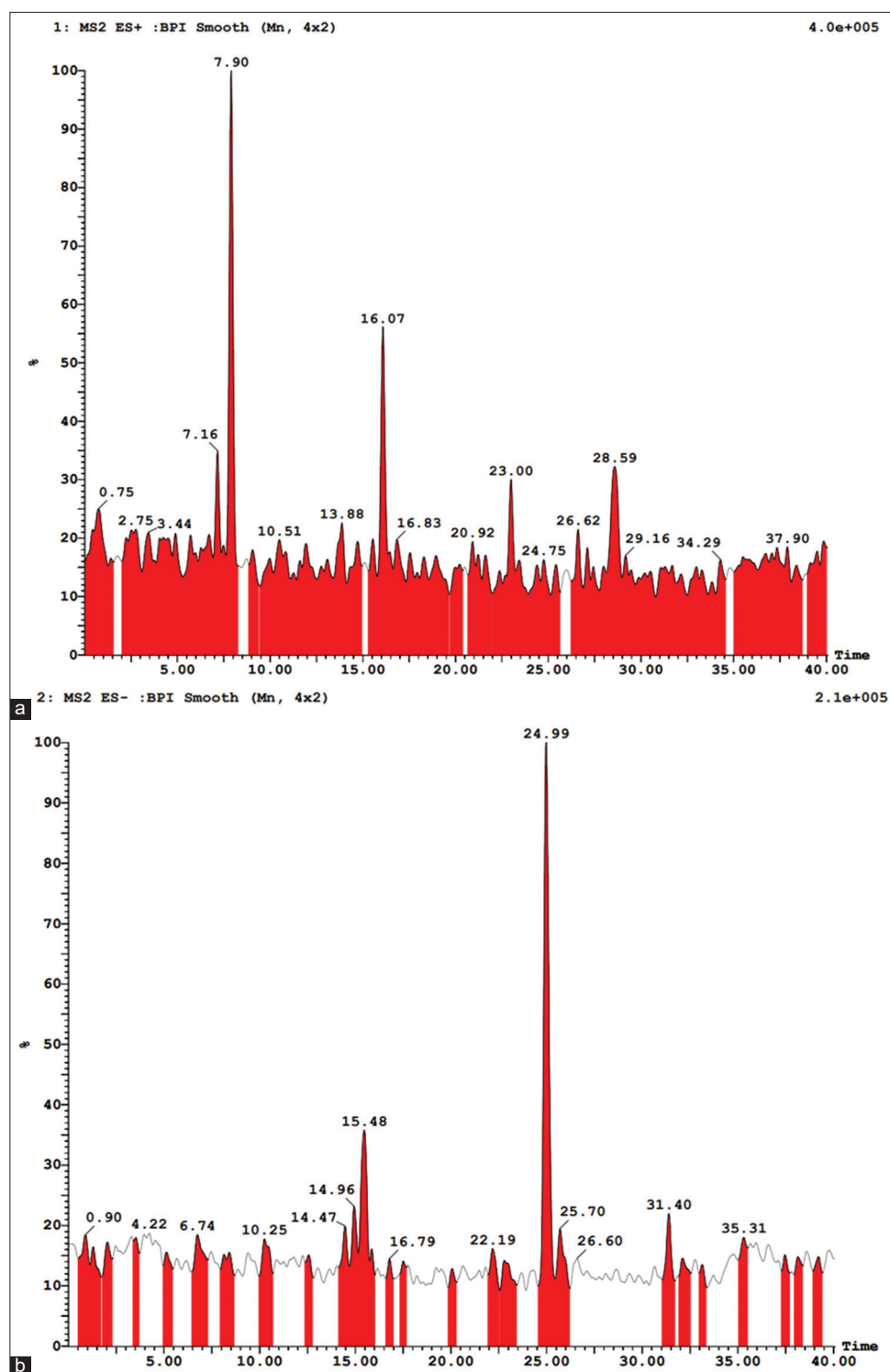


Fig. 3: Liquid chromatography-mass spectrometry data (a) positive and (b) negative ion mode of chloroform extract of *Urochloa distachya*

Molecular docking

Molecular docking studies were conducted to investigate the anti-inflammatory activities of compounds from CUD and EAUD, which were identified by GC-MS and LC-MS analysis. In this investigation, 38 compounds were docked into the binding sites of COX-2 (3 mdl), 5-LOX (6 ncf), PDE4 (4 wcu), and HP5 (1 hd2). The docking score revealed that all ligands showed activity ranging from -4.3 to -15.3 against COX-2, -4.6--13.6 against 5-LOX, -3.9--17.1 against PDE4, and -3.9--11.6 against HP5 (Tables 6 and 7). According to their overall docking score, the drugs exhibited relatively superior binding efficacy against

COX-2 and PDE4 compared to two other target receptors. The docking score, hydrogen bond interacting residues, and distance between the interaction of ligands are given in Tables 6 and 7, and the 2D and 3D structures of interacted molecules are illustrated in Figs. 9-14.

DISCUSSION

The GC-MS and LC-MS investigations of CUD and EAUD identified a variety of bioactive compounds that provide strong evidence for the observed anti-inflammatory and other therapeutic activities in the

Table 4: LC-MS analysis of positive (M+H)⁺, and negative (M-H)⁻ ion mode of EAUD

Sl. No.	Name of the compound	Nature	M.F.	M.W.	Biological activity	References
1	2,4,5,6-Tetrachloro nicotinamide	Vitamin	C ₆ H ₄ Cl ₄ N ₂ O	257.89	Not reported	
2	2-Acetamido-1,5-anhydro-2-deoxyhex-1-enitol	-	C ₈ H ₁₃ NO ₅	203.08	Not reported	
3	2-Cyclohexyl-2-hydroxyacetamide	-	C ₈ H ₁₅ NO ₂	157.11	Not reported	
4	Pyrogallol	Phenolic	C ₆ H ₆ O ₃	126.03	Antibacterial activity. Inhibitor for anticholinesterase.	[92,93]
5	1-Allyl-2-benzyl-1,2-dihydropyridine	-	C ₁₅ H ₁₇ N	211.14	Not reported	
6	(4aR,4bR,8S,10aR,10bR,12aS)-8-Hydroxy-10a, 12a-dimethyl-3,4,4a, 4b, 5,7,8,9,10,10a, 10b, 11,12,12a-tetradecahydronaphtho[2,1-f] quinolin-2 (1H)-one	-	C ₁₉ H ₂₃ NO ₂	303.22	Not reported	
7	4-[5-Acetoxy-8,8-dimethyl-6-(3-methyl-2-buten-1-yl)-4-oxo-4H,8H-pyrano[2,3-f] chromen-3-yl]-1,2-phenylene diacetate	-	C ₃₁ H ₃₀ O ₉	546.19	Not reported	
8	NP-008993	Fatty acid	C ₂₀ H ₄₀ O ₅	360.29	Not reported	
9	Oleamide	Natural agonist	C ₁₈ H ₃₅ NO	281.27	Inhibit cellular triglyceride in the hepatocytes.	[94]
10	9-Oxo-10(E),12(E)-octadecadienoic acid	-	C ₁₈ H ₃₀ O ₃	294.22	Not reported	
11	2-Methoxy-N, N-diundecylacetamide	-	C ₂₅ H ₅₁ NO ₂	397.39	Not reported	[95]
12	2-Aminoadipic acid	Alpha-amino acid	C ₆ H ₁₁ NO ₄	161.07	Anti-inflammatory, neuroprotective activity.	
13	Hexyl 2-propylheptyl phthalate	Organic compound	C ₂₄ H ₄₀ O ₄	390.28	Not reported	
14	N, N'-ethylenebis palmitamide	Organic compound	C ₃₀ H ₅₈ N ₂ O ₂	536.53	Not reported	
15	N-2-Propyn-1-ylcysteine	Organic compound	C ₆ H ₉ NO ₂ S	159.03	Not reported	
16	D-(-)-Mannitol	Sugar alcohol	C ₆ H ₁₂ N ₂ OP ₂	181.98	Cerebral edema, decreased intra-ocular pressure, diuresis, reduced renal cell swelling.	[88]
17	3-hydroxy-2-([(2E)-3-(4-hydroxyphenyl) prop-2-enoyl] oxy)-3-(methoxycarbonyl) pentanedioic acid	-	C ₂₈ H ₂₄ N ₁₀ O ₄	564.20	Not reported	
18	4-Undecylbenzenesulfonic acid	Arenesulfonic acid	C ₁₇ H ₂₈ O ₃ S	312.18	Not reported	
19	Tetradecyl N-(ethoxycarbonyl) alaninate	-	C ₂₀ H ₃₈ N ₂ O ₄	357.29	Note reported	
20	Glycol stearate	Organic compound	C ₂₀ H ₄₀ O ₃	328.30	Emulsifying agent.	[91]
21	Methyl 12-hydroxystearate	Fatty acid	C ₁₉ H ₃₈ O ₃	314.28	Textile ancillary, cosmetics, and paper industry	[96]
22	NP-021293	-	C ₅ H ₉ O ₆ PS	259.92	Note reported	

LC-MS: Liquid chromatography-mass spectrometry, EAUD: Ethyl acetate extracts of *Urochloa distachya*

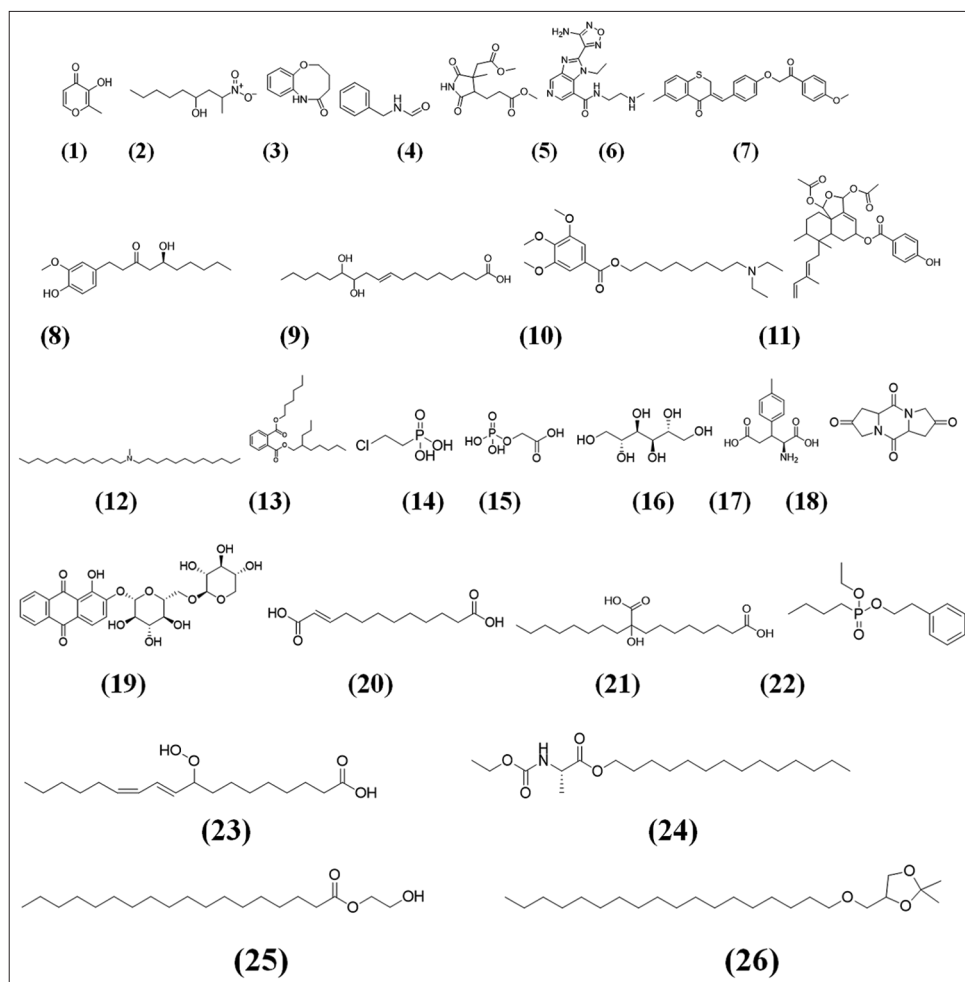


Fig. 4: Structure of the compounds from liquid chromatography-mass spectrometry analysis of positive (M+H)⁺ and negative (M-H)⁻ ion mode of chloroform extract of *Urochloa distachya*

Table 5: *In vivo* anti-inflammatory activity

Group	Treatment	Change in paw thickness (mm)±SD (% inhibition)			
		1 st h	2 nd h	3 rd h	4 th h
Group I: Carrageenan Control	Carrageenan induced (0.1 mL of 1% w/v)	2.17±0.12	2.60±0.14	3.42±0.12	3.07±0.10
Group II: Positive Control	Carrageenan induced (0.1 mL of 1% w/v)+Indomethacin 10 mg/kg b.w.	1.24±0.03 ^{a*}	1.29±0.01 ^{a*}	0.85±0.15 ^{a*}	0.50±0.13 ^{a*}
Group III: Test-1	Carrageenan induced (0.1 mL of 1% w/v)+Indomethacin 10 mg/kg b.w.	43.09%	50.32%	75.15%	83.7%
	Carrageenan induced (0.1 mL of 1% w/v)+CUD 400 mg/kg b.w.	1.67±0.02 ^{b*}	1.77±0.01 ^{b*}	1.44±0.02 ^{b*}	1.29±0.02 ^{b*}
Group IV Test-2	Carrageenan induced (0.1 mL of 1% w/v)+CUD 400 mg/kg b.w.	22.89%	31.80%	57.89%	57.9%
	Carrageenan induced (0.1 mL of 1% w/v)+EAUD 400 mg/kg b.w.	2.05±0.03 ^{c*}	2.45±0.03 ^{c*}	2.34±0.02 ^{c*}	2.26±0.03 ^{c*}
		5.38%	5.64%	31.73%	26.5%

The data are expressed as standard error mean (n=6). The values were carried out by One-way analysis of variance (Tukey's test). a*, b*, and c* = p<0.05 compared to carrageenan control group. CUD: Chloroform extract of *Urochloa distachya*, EAUD: Ethyl acetate extract of *Urochloa distachya*

study. Triamcinolone Acetonide, a corticosteroid identified in the GC-MS analysis, is known for its wide range of therapeutic effects, including anti-inflammatory, analgesic, and immunosuppressive activities, making it useful for conditions such as rheumatoid arthritis, Addison's disease, leukemia, and various allergic reactions [64-66]. Campesterol, another steroidal compound, exhibited not only anti-inflammatory effects but also cytotoxic, antioxidant, anticancer, and antibacterial properties, highlighting its therapeutic versatility [48,67,68]. The alcoholic compound 7,8-Epoxylostan-11-ol, 3-acetoxy-, showed anti-inflammatory and antimicrobial activities [71,72], whereas Epoxycholesterol demonstrated pro-inflammatory and cytotoxic effects, as well as a role in cholesterol efflux regulation

[76,77]. Fluprednisolone, a steroid, is well-established for its anti-inflammatory activity, contributing to the study's findings [80].

The LC-MS analysis revealed Maltol, an organic compound with a broad spectrum of biological activities, including antimicrobial, anti-inflammatory, antioxidant, and anticancer effects, making it valuable for cosmetic and therapeutic applications [83,84,97,98]. 6-Gingerol, a phenolic compound, showed potent anti-inflammatory, antioxidant, and anticancer properties [85], whereas 2-Aminoadipic acid, an alpha-amino acid, exhibited anti-inflammatory and neuroprotective activities. Collectively, these compounds considerably improve the study's findings on the anti-inflammatory potential of CUD

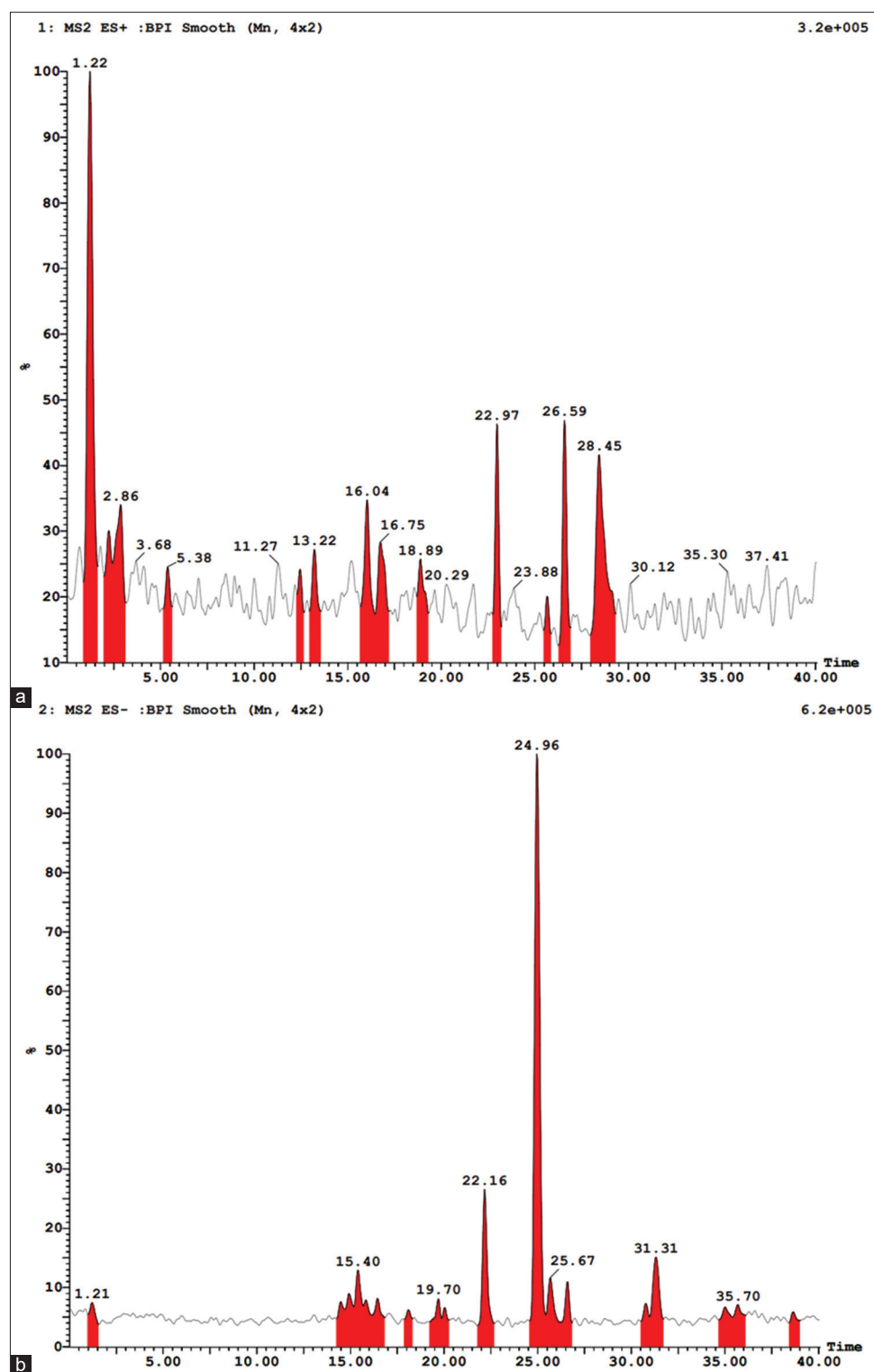


Fig. 5: Liquid chromatography-mass spectrometry data (a) positive and (b) negative ion mode of ethyl acetate extracts of *Urochloa distachya*

and EAUD, thereby further supporting their diverse therapeutic applications.

Inflammation is a complex process that results from a severe disruption in tissue homeostasis [99]. The paw edema resulting from carrageenan is a biphasic phenomenon. The initial phase, occurring within the 1st h post-injection, is driven by the release of histamine, serotonin, and kinins. The second phase, beginning at the end of the first and lasting

2-3 h, is predominantly mediated by prostaglandin [100]. The *in vivo* anti-inflammatory potential of both CUD and EAUD was assessed using the carrageenan-induced paw edema model. The findings showed that CUD had better anti-inflammatory properties relative to EAUD. The CUD-treated group exhibited a notable decrease in paw edema, especially in the later stages of inflammation, indicating that CUD effectively suppressed both the initial and later phases of the inflammatory response. On the other hand, EAUD exhibited anti-inflammatory

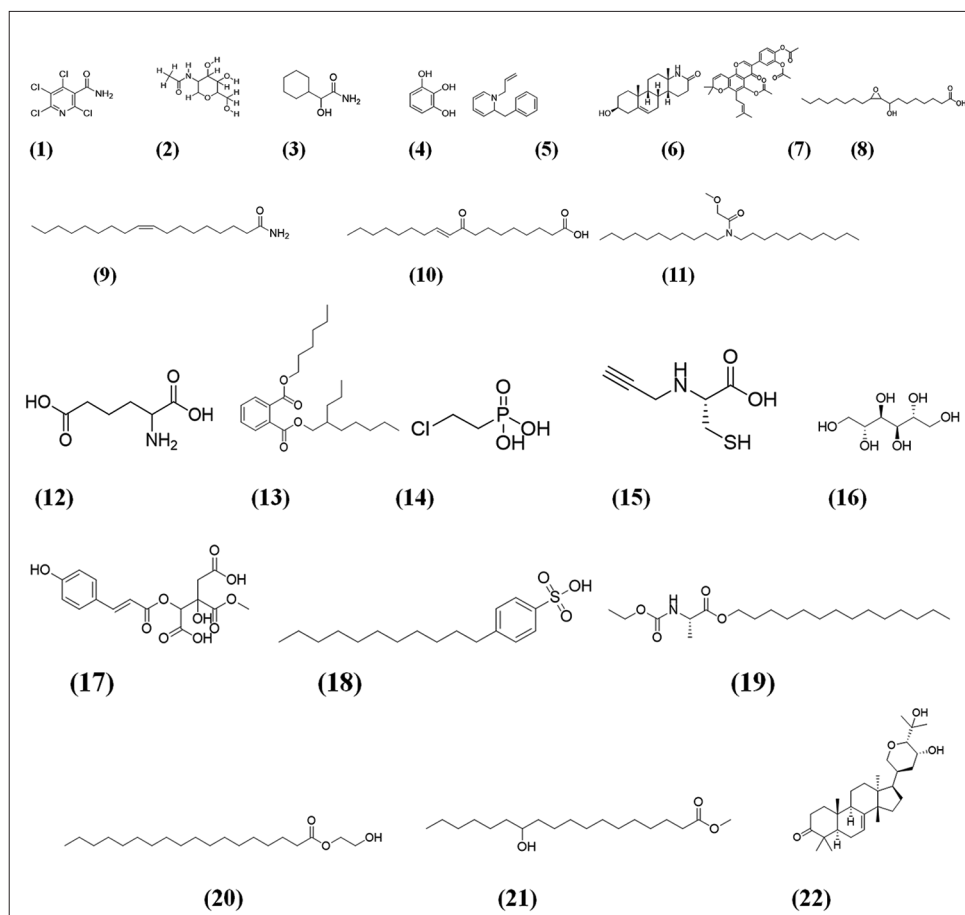


Fig. 6: Structure of the compounds from liquid chromatography-mass spectrometry analysis of positive (M+H)⁺, and negative (M-H)⁻ ion mode of ethyl acetate extracts of *Urochloa distachya*

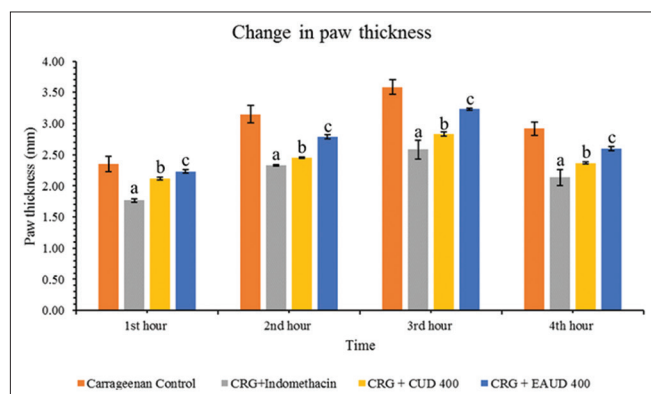


Fig. 7: Change in paw edema by 400 mg/kg b.w. of chloroform extract of *Urochloa distachya* and ethyl acetate extracts of *U. distachya* in rats induced with carrageenan

activity but yielded a comparatively lesser response, indicating that the compounds found in CUD may possess a more reliable or sustained effect in mitigating inflammation. The findings indicate that CUD possesses significant potential as an anti-inflammatory effect.

Anodendroside E 2, Triamcinolone Acetonide, Fluprednisolone, Maltol, 6-Gingerol, and 2-Aminoadipic acid were identified through GC-MS and LC-MS analyses of the CUD and EAUD, demonstrating notable anti-inflammatory activity. In this study, molecular docking analysis was performed to evaluate the binding capacity of these compounds with inflammatory targets such as COX-2, 5-LOX, PDE4, and HP5.

A hydrogen bond forms between the nitrogen atom of the imidazole side chain of histidine (HIS)351 and the oxygen atom of Anodendroside E 2. This interaction stabilizes the compound at the COX-2 active site. The hydrogen bond forms between the amide side chain of glutamine (GLN)565 and a hydroxyl group on Anodendroside E 2, enhancing its binding affinity. Two hydrogen bonds are established between the primary nitrogen atoms of glycine (GLY)354 and two oxygen atoms of Anodendroside E 2, highlighting the dual interaction locations with this residue. The hydroxyl group of threonine (THR)94 establishes a hydrogen bond with an oxygen atom in the molecule, enhancing the stability of the contact within the binding pocket. The oxygen atoms (O) of hydroxyl (-OH), ester, or carbonyl groups in Anodendroside E 2 are probably engaging in hydrogen bond formation with the hydrogen atoms of the amino acid side chains (Serine [SER]171, GLN611, GLU622) in the enzyme 5-LOX. In the interaction between Anodendroside E 2 and PDE4. Asparagine (ASN)209 forms two hydrogen bonds with Anodendroside E 2 at distances of 2.03 Å and 2.22 Å, likely involving the oxygen atoms of the hydroxyl or carbonyl groups on the ligand. These short distances indicate strong hydrogen bonds. GLN210 forms a weaker hydrogen bond at a distance of 3.22 Å, likely interacting with an oxygen atom of the ligand's hydroxyl or ester groups. Aspartic acid (ASP)318 also forms a weaker hydrogen bond at a distance of 3.39 Å, probably involving its carboxyl group interacting with an oxygen atom from Anodendroside E 2. In the interaction between Anodendroside E 2 and HP-5, two key residues are involved in hydrogen bonding. ASN21 forms a hydrogen bond with an oxygen atom of Anodendroside E 2 at a distance of 2.12 Å, indicating a strong interaction. GLU16 also forms a hydrogen bond at a slightly longer distance of 2.76 Å, likely involving the hydrogen atom attached to the hydroxyl group of Anodendroside E 2. The 3D and 2D interactions are illustrated in Fig. 9.

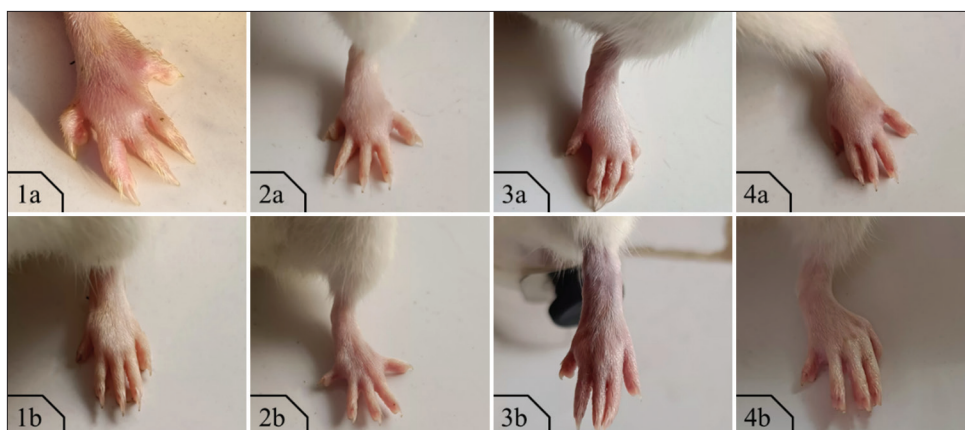


Fig. 8: Effect of carrageenan, indomethacin, chloroform extract of *Urochloa distachya* (CUD), and ethyl acetate extracts of *U. distachya* (EAUD) on the left hind paw of rats at 1 h and 4 h. (1a and b) showed the effect of carrageenan induced (0.1 mL of 1% w/v). (2a and b) showed the effect of indomethacin 10 mg/kg b.w. (3a and b) showed the effect of carrageenan induced (0.1 mL of 1% w/v)+CUD 400 mg/kg b.w. (4a and b) showed the effect of carrageenan induced (0.1 mL of 1% w/v)+EAUD 400 mg/kg b.w

Table 6: Binding energies (Kcal/mol) of phytochemicals identified through GC-MS and LCMS analysis of CUD and EAUD assessed for anti-inflammatory potential via molecular docking studies

Sl. No	Name of the compound	COX-2 (3 mdl)	5-LOX (6 ncf)	PDE4 (4 wcu)	HP5 (1 hd2)
1	Indomethacin	-6.7	-7.1	-9.6	-6.5
2	Triamcinolone Acetonide	-8.3	-8.2	-9.5	-6.4
3	Campesterol	-7.4	-7.5	-8.7	-6.9
4	Docosanoic acid, 1,2,3-propanetriyl ester	-5.7	-3.1	-6.3	-3.5
5	7,8-Epoxy lanostan-11-ol, 3-acetoxy-	-8.6	-7.8	-7.9	-6.7
6	Anodendroside E 2	-10.3	-9.3	-10.7	-7.9
7	7,8,12-Tri-O-acetyl-3-desoxy-ingol-3-one	-11.6	-9.9	-12.5	-8.6
8	9-Octadecenoic acid (Z)-, 3-[(1-oxohexadecyl) oxy]-2-[(1-oxooctadecyl) oxy] propyl ester	-5.1	-5.2	-6.3	-3.4
9	Epoxycholesterol	-7.3	-6.9	-8.7	-6.4
10	Holothurin acetate	-15.3	-13.6	-17.1	-11.6
11	Octadecanoic acid, 1-[[[(1-oxohexadecyl) oxy] methyl]-1,2-ethanediyl ester	-6.5	-6.3	-6.5	-3.1
12	Fluprednisolone	-7.9	-7.3	-9.5	-6.5
13	(±) 9-HpODE	-6.9	-6.2	-6.7	-5.2
14	(±) 12 (13)-DiHOME	-6.9	-6.2	-5.9	-5.2
15	2-(4-Amino-1,2,5-oxadiazol-3-yl)-1-ethyl-N-[2-(methylamino) ethyl]-1H-imidazo[4,5-c] pyridine-7-carboxamide	-7.2	-7.1	-7.3	-6.4
16	2,2-Dimethyl-4-[(octadecyloxy) methyl]-1,3-dioxolane	-6.7	-7.4	-7.5	-5.4
17	2-Hydroxy-2-octyldecanedioic acid	-6.9	-7.7	-7.5	-5.6
18	2-Nitro-4-nonanol	-6.1	-5.6	-5.6	-4.5
19	3-(4-Methylphenyl) glutamic acid	-6.3	-6.4	-6.9	-5.7
20	3,4-Dihydro-2H-1,6-benzoxazocin-5 (6H)-one	-7.4	-7.5	-6.9	-5.6
21	6-Gingerol	-6.7	-6.5	-6.9	-5.2
22	Dihydro-1H,5H-dipyrrolo[1,2-a:1',2'-d] pyrazine-2,5,7,10 (3H,8H,10aH)-tetrone	-7.7	-6.6	-7.3	-5.7
23	Ethephon	-4.3	-4.6	-3.9	-3.9
24	Ethyl 2-phenylethyl butylphosphonate	-7.1	-7.3	-6.3	-4.6
25	Maltol	-5.7	-5.7	-5.4	-4.7
26	Methyl 3-[4-(2-methoxy-2-oxoethyl)-4-methyl-2,5-dioxo-3-pyrrolidinyl] propanoate	-5.9	-5.9	-6.5	-5.5
27	N-Benzylformamide	-6.2	-6.1	-6.6	-4.7
28	Phosphoglycolate	-5.0	-4.8	-4.8	-4.6
29	TMB-8	-7.3	-7.3	-7.3	-6.3
30	Traumatic Acid	-6.3	-4.9	-5.8	-5.3
31	2-Aminoadipic acid	-5.7	-5.2	-5.5	-4.7
32	2-Cyclohexyl-2-hydroxyacetamide	-6.9	-5.8	-6.6	-5.2
33	4-Undecylbenzenesulfonic acid	-6.5	-4.9	-6.7	-5.4
34	9-Oxo-10(E),12(E)-octadecadienoic acid	-6.3	-6.4	-6.7	-5.3
35	Methyl 12-hydroxystearate	-7.1	-6.5	-6.5	-5.0
36	NP-008993	-6.5	-5.9	-6.5	-5.4
37	Oleamide	-6.8	-5.8	-6.0	-4.7
38	Pyrogallol	-5.8	-5.4	-5.3	-5.3

LC-MS: Liquid chromatography-mass spectrometry, EAUD: Ethyl acetate extracts of *Urochloa distachya*, CUD: chloroform extract of *Urochloa distachya*

Table 7: Hydrogen bond, amino acid residue, and interaction distance of phyto-compounds from GC-MS analysis of CUD and EAUD

Sl. No.	Name of the compound	COX-2 (3 mdl)		5-LOX (6 ncf)		PDE4 (4 wcu)		HP5 (1 hd2)	
		Hydrogen bonds	Distance (Å)	Hydrogen bonds	Distance (Å)	Hydrogen bonds	Distance (Å)	Hydrogen bonds	Distance (Å)
1	Indomethacin	HIS351, LYS358, ASP347, GLN350	1.77, 2.19, 2.72, 3.99	GLU16, ASP170	2.14, 3.73	SER368	3.29	GLU91, GLY92, LYS93, GLY82	2.34, 1.92, 2.78, 2.22
2	Anodendroside E 2	HIS351, GLN565, GLY354, GLY354, THR94	1.95, 1.85, 3.49, 3.67, 3.26	SER171, GLN611, GLU622	2.62, 2.47, 2.46	ASN209, ASN209, ASP318, GLN210	2.03, 2.22, 3.39, 3.22	ASN21, GLU16	2.12, 2.76
3	Campesterol	-	-	LYS83	3.46	-	-	GLU83	2.06
4	Triamcinolone Acetonide	HIS351, GLN565, GLN350, GLY354, SER579	2.67, 2.48, 2.22, 3.41, 3.50	ARG401, ASN613	2.82, 2.07	HIS160, HIS204, ASN209, THR271, GLU230, HIS160	2.72, 2.30, 2.82, 2.38, 2.51, 3.56	GLU91, ARG95	2.43, 3.63
5	Epoxysterol	PRO191	3.00	-	-	HIS160, ASP318, HIS200	2.50, 2.68, 3.64	-	-
6	Fluprednisolone	HIS356, GLN565, HIS356, ASP347	3.56, 2.38, 3.60, 3.56	ASP170	2.59	HIS204, VAL207	2.73, 2.62	GLY92, ARG95, GLY85, GLU91	2.19, 2.65, 3.50, 3.28
7	(±) 9-HpODE	MET522, VAL523	2.32, 2.95	TYR470, GLN549, LEU448	3.07, 2.33, 2.82	THR333, HIS164, HIS200, ASP318	3.12, 3.06, 2.92, 2.04	ASN21, ARG86, ALA90, VAL94, GLY17, GLY17, ARG95	2.32, 3.08, 2.32, 2.35, 3.50, 3.62, 3.46
8	(±) 12 (13)-DiHOME	-	-	TYR81, TYR100	2.60, 2.95	TYR159	3.36	LYS63, LYS63, LYS63, LEU96, GLU16, VAL70	1.95, 2.46, 2.46, 1.89, 2.54, 2.91
9	2-(4-Amino-1,2,5-oxadiazol-3-yl)-1-ethyl-N-[2-(methylamino)ethyl]-1H-imidazo[4,5-c]pyridine-7-carboxamide	ASN537, GLY225, ASN375	2.30, 1.96, 3.77	GLN141, LYS161, ASP162, GLN141	2.72, 1.90, 2.80, 3.12	TYR159, GLN343	2.74, 2.25	ASN21, GLY92, GLU91, GLY82	2.61, 3.00, 2.51, 2.52
10	2,2-Dimethyl-4-[[octadecyloxy]methyl]-1,3-dioxolane	GLU465	3.64	-	-	HIS160, GLU230	2.37, 3.36	ARG95	3.28
11	2-Nitro-4-nonanol	THR206, HIS386, HIS388, TYR385	2.39, 3.50, 3.72, 3.29	HIS624, ASP166	2.29, 2.90	TYR159, HIS160, HIS164	2.13, 2.14, 3.56	ARG95	3.75
12	3-(4-Methylphenyl) glutamic acid	GLN350, HIS351, LYS358	2.99, 2.84, 2.28	GLN611	2.39	ASP318, HIS160	2.72, 3.49	LEU96, GLY82, GLY17, ARG95, LU91	2.06, 2.16, 3.59, 3.51, 2.53
13	3,4-Dihydro-2H-1,6-benzoxazocin-5(6H)-one	SER530	2.48	-	-	TYR159	2.49	GLY17	3.50
14	6-Gingerol	ARG44, CYS41	2.05, 2.42	GLN611, GLN611, ARG401, GLU614	2.74, 2.18, 2.65, 1.94, 3.30	HIS160, ASN321	2.26, 3.57	GLY92, LEU96	2.63, 1.99
15	Dihydro-1H,5H-dipyrrolo[1,2-a1',2'-d]pyrazine-2,5,7,10 (3H,8H,10aH)-tetrone	LYS468, ARG44	3.25, 3.31	SER447	3.69	TYR159, HIS160, ASP318	2.63, 2.40, 3.38	LEU96, GLY82	3.18, 3.65, 3.75
16	Ethyl 2-phenylethyl butylphosphonate	ALA527	3.28	HIS367	2.43	HIS160	2.34	-	-
17	Maltol	HIS207	2.77	PRO565	3.28	-	-	GLU91, GLY82, LEU96	2.12, 2.48, 2.06
18	Methyl 3-[4-(2-methoxy-2-oxoethyl)-4-methyl-2,5-dioxo-3-pyrrolidinyl]propanoate	LYS83, TYR115, SER119	2.47, 2.47, 1.94	GLN141, ARG165, ASP166, GLN168, ASP166, THR104	2.45, 2.56, 2.53, 3.02, 3.09, 3.79	TYR159, THR333	2.74, 3.74	ASN21, ASN21, GLU91, GLY92, GLU91	2.49, 2.47, 2.35, 2.46, 3.11

(Contd...)

Table 7: (Continued)

Sl. No.	Name of the compound	COX-2 (3 mdl)		5-LOX (6 ncf)		PDE4 (4 wcu)		HP5 (1 hd2)	
		Hydrogen bonds	Distance (Å)	Hydrogen bonds	Distance (Å)	Hydrogen bonds	Distance (Å)	Hydrogen bonds	Distance (Å)
19	N-Benzylformamide	HIS207, TYR385	2.74, 2.64	ILE404, ALA405, TYR383	2.10, 2.21, 2.86	THR333, ASN321	3.25, 2.77	GLY92, GLU16	2.36, 2.51
20	Phosphoglycolate	HIS207, HIS388, ASN382, ASN382	2.38, 2.81, 2.73, 2.00	TRP102, TYR81, TYR100, TYR100, ASP166, GLN168	2.14, 2.31, 2.29, 2.16, 2.12, 2.82	HIS204, THR27, HIS164, ASP201, GLU230	1.98, 2.45, 2.80, 1.99, 2.66	GLY17	3.58
21	Traumatic Acid	TYR355	1.84	ASP285	2.78	HIS160, TRP332	2.46, 3.10	LXS63, LXS63, LXS63, LXS63, LXS63, LXS63, GLU91, LYS93	2.72, 2.49, 2.65, 2.98, 2.65, 2.98, 2.13, 2.44
22	2-Aminoadipic acid	THR206, HIS207, TYR385	2.98, 2.54, 2.41	TRP102, HIS624, ASP166, TYR383, TYR81, TYR100	2.23, 2.17, 2.99, 2.70, 2.34, 2.41	TYR159, HIS160, ASP318, ASP318	2.35, 2.22, 2.33, 2.16	LXS63, LXS63, LXS63, LXS63, LXS63, LXS63, VAL70, GLY92, GLN68	2.62, 2.60, 2.17, 2.93, 2.17, 2.93, 2.34, 2.51, 2.15
23	2-Cyclohexyl-2-hydroxyacetamide	THR206, HIS207, TYR385	3.26, 2.32, 2.83	HIS624, TYR81, TYR100, TYR100	2.39, 2.72, 1.95, 2.45	HIS160, ASP318, ASP318, ASP318	2.41, 2.52, 2.16, 2.79, 2.17	GLY92, GLU16, GLU91	2.67, 2.18, 3.24
24	4-Undecylbenzenesulfonic acid	TRP387, HIS388	2.38, 3.61	-	-	HIS204, ASP201	2.39, 2.38	LXS63, LXS63, LXS63, LXS63, GLY92	2.15, 2.73, 2.52, 2.49, 2.71
25	9-Oxo-10(E),12(E)-octadecadienoic acid	ARG222, PHE210	3.36, 2.45	LEU448, THR545, SER447	2.50, 2.35, 3.65	GLN433, THR333	2.63, 2.52	LXS63, LXS63, LXS63, LXS63, VAL70	2.74, 2.53, 2.68, 3.00, 2.68, 3.00, 2.77
26	Oleamide	HIS207, THR206	2.38, 2.70	-	-	HIS160, HIS204, ASP201	2.65, 2.26, 2.19	LXS63, LXS63, LXS63, VAL70, VAL70, LYS93	2.18, 2.55, 2.55, 2.63, 2.86, 2.52
27	Pyrogallol	-	-	THR545, ARG370	2.99, 4.05	-	-	LXS63, LXS63, LXS63, GLY92, VAL70, GLY92	2.45, 2.79, 2.37, 2.02, 2.02, 2.20, 2.18, 2.86

ALA: Alanine, ARG: Arginine, ASN: Asparagine, ASP: Aspartic acid, GLN: Glutamine, GLU: Glutamic acid, GLY: Glycine, HIS: Histidine, LEU: Leucine, LYS: Lysine, MET: Methionine, PHE: Phenylalanine, PRO: Proline, SER: Serine, THR: Threonine, TRP: Tryptophan, TYR: Tyrosine, VAL: Valine

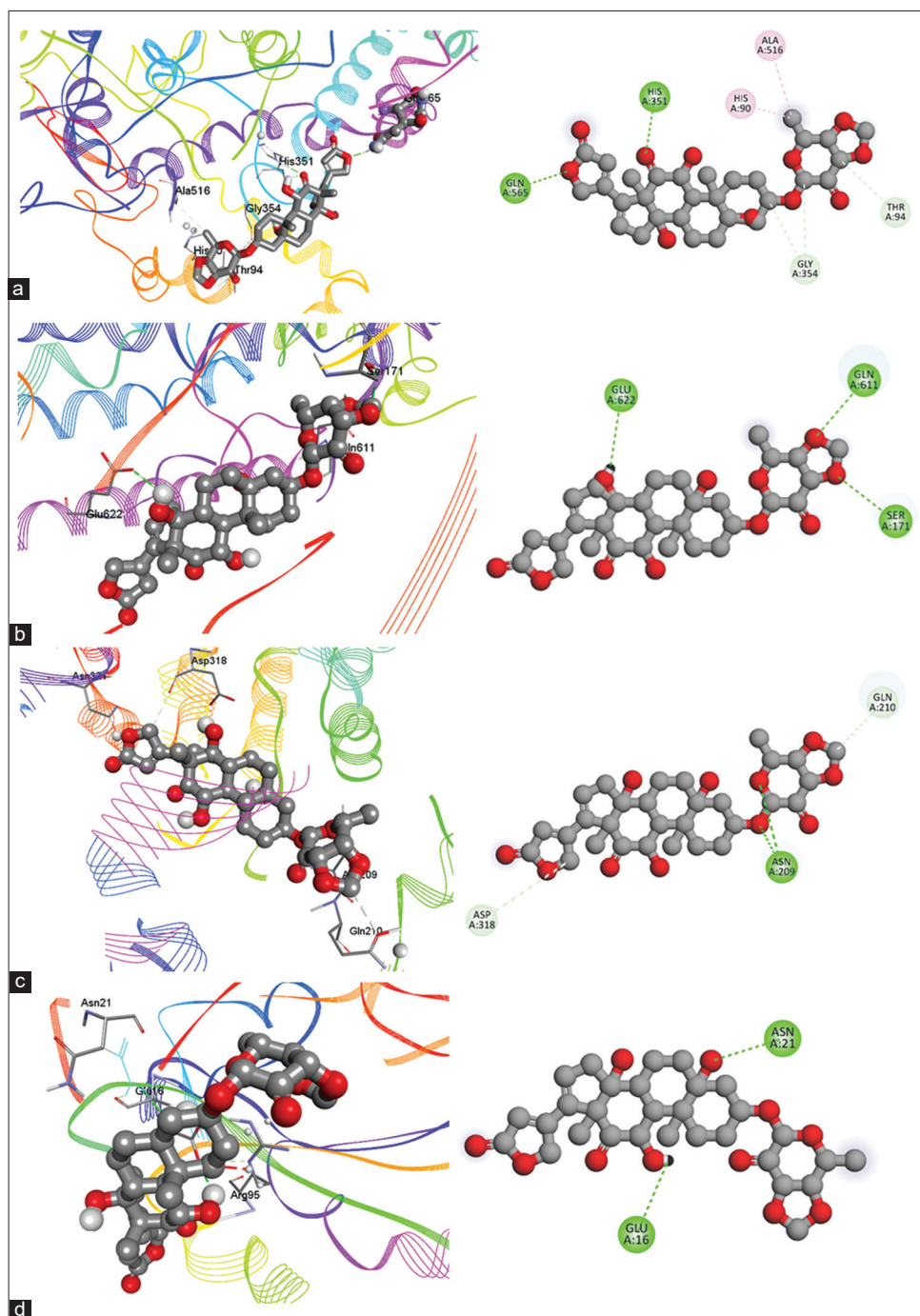


Fig. 9: Molecular interactions and binding affinities of Anodendroside E 2 with (a) cyclooxygenase-2, (b) 5-lipoxygenase, (c) Phosphodiesterase 4, and (d) Human peroxiredoxin 5

The hydrogen bond interactions between Triamcinolone Acetonide and COX-2 occur through specific atoms of both the ligand and the enzyme's amino acid residues. In the case of HIS351, the nitrogen atom in the imidazole ring interacts with a hydrogen donor from the ligand, forming a bond at 2.67 Å. For GLN565, the carbonyl oxygen of Triamcinolone Acetonide interacts with the amide nitrogen of the residue, with a bond length of 2.48 Å. GLN350 forms a hydrogen bond at 2.22 Å, where the oxygen atom of the ligand's hydroxyl group interacts with the amide nitrogen of the residue. GLY354 is involved through its backbone amide group interacting with an oxygen atom from the ligand, at a distance of 3.41 Å. Finally, SER579 forms a hydrogen bond at 3.50 Å, where the hydroxyl oxygen of the SER side chain interacts with the carbonyl group of Triamcinolone

Acetonide. In the case of Arginine (ARG)401, the guanidinium group of ARG interacts with an oxygen atom from the carbonyl group of Triamcinolone Acetonide, forming a hydrogen bond at 2.82 Å. For ASN613, the side chain amide group interacts with a hydroxyl group of the ligand at a distance of 2.07 Å. These atomic interactions stabilize the binding of Triamcinolone Acetonide in the active site of 5-LOX, enhancing its inhibitory effect on the enzyme. The hydroxyl groups and carbonyl oxygen atoms of Triamcinolone Acetonide are key interaction sites with the nitrogen atoms of HIS residues (HIS160, HIS204), amide groups of ASN209, hydroxyl groups of THR271, and the carboxyl group of GLU230. The molecular interactions between Triamcinolone Acetonide and HP-5 are primarily stabilized by a strong hydrogen bond with GLU91 (2.43 Å) and a weaker hydrogen

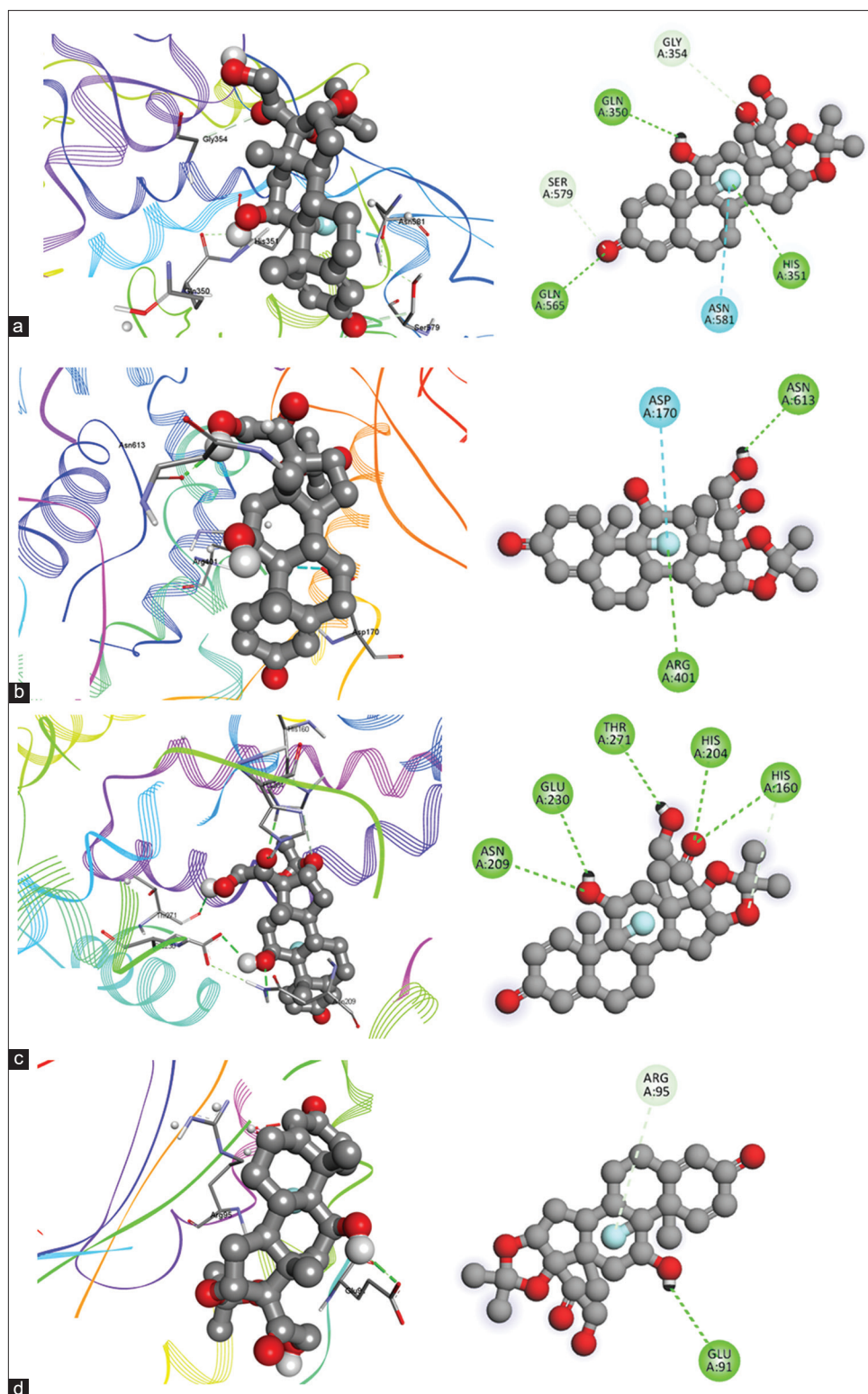


Fig. 10: Molecular interactions and binding affinities of Triamcinolone Acetonide with (a) cyclooxygenase-2, (b) 5-lipoxygenase, (c) Phosphodiesterase 4, and (d) Human peroxiredoxin 5

bond with ARG95 (3.63 Å). The 3D and 2D interactions are depicted in Fig. 10.

The interaction between Fluprednisolone and COX-2, HIS356, forms two hydrogen bonds with Fluprednisolone at distances of 3.56 Å and 3.60 Å, indicating relatively weaker interactions. GLN565 forms a strong hydrogen bond at a distance of 2.38 Å, likely involving the

oxygen atom from the carbonyl or hydroxyl group of Fluprednisolone interacting with the amide group of GLN565. ASP347 forms a hydrogen bond at a distance of 3.56 Å, involving its carboxyl group interacting with an oxygen atom from Fluprednisolone. The interaction between Fluprednisolone and 5-LOX indicates a moderately strong interaction, likely involving the carboxyl group of ASP170 and a hydroxyl or carbonyl group on Fluprednisolone. In the interaction between

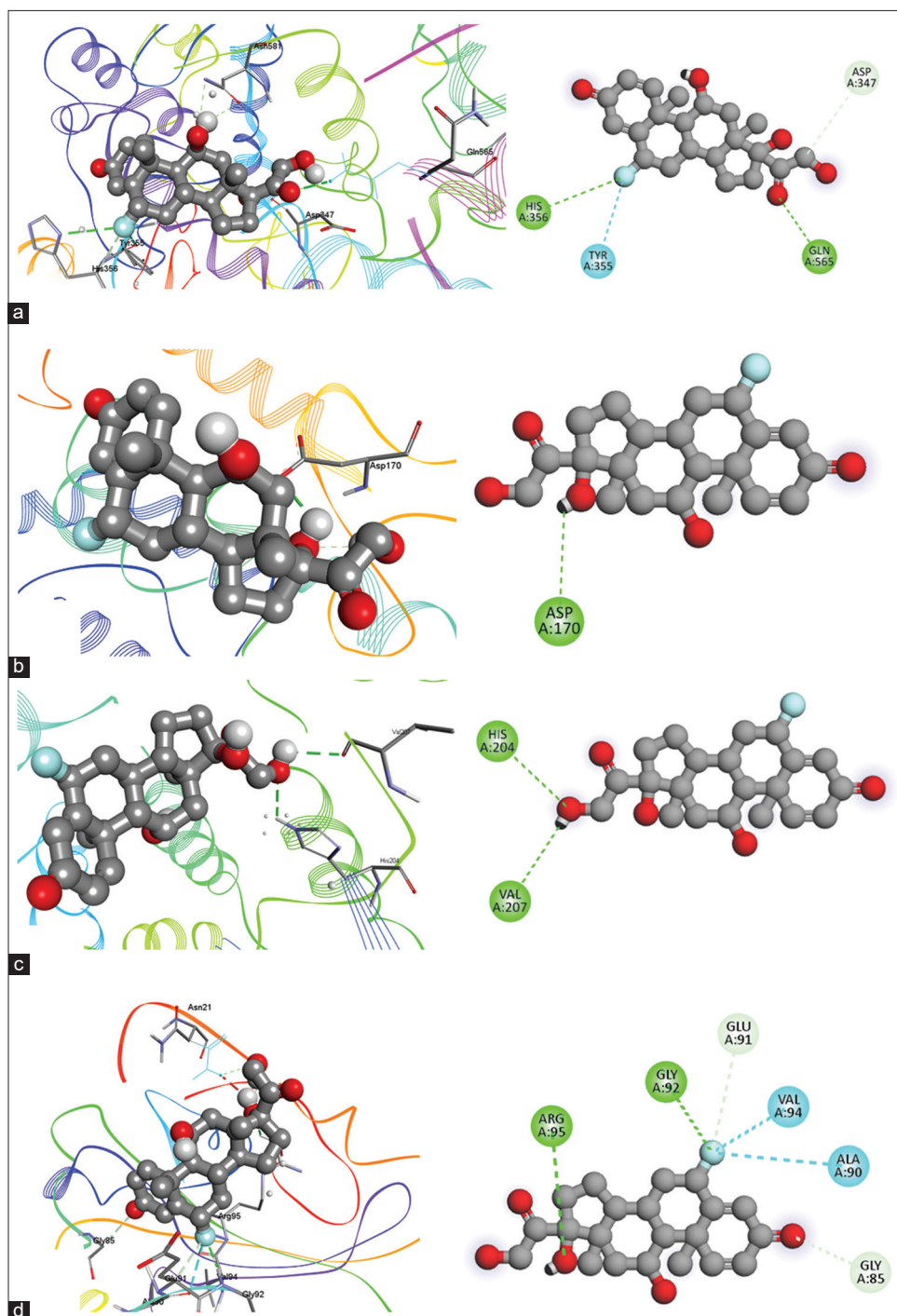


Fig. 11: Molecular interactions and binding affinities of Fluprednisolone with (a) cyclooxygenase-2, (b) 5-lipoxygenase, (c) Phosphodiesterase 4, and (d) Human peroxiredoxin 5

Fluprednisolone and PDE4, the interactions likely involve a hydroxyl group on Fluprednisolone engaging with the side chains of HIS204 and valine (VAL)207, contributing to the stabilization of the ligand within the PDE4 binding pocket. The interaction between Fluprednisolone and HP-5 involves key hydrogen bond interactions with several residues such as GLY92, ARG95, GLY85, and GLU91. The 3D and 2D interactions are depicted in Fig. 11.

The interaction between Maltol and COX-2 is mediated primarily through a hydrogen bond with the HIS207 residue. The imidazole nitrogen atom of HIS207 forms a hydrogen bond with the carbonyl

oxygen atom of Maltol at a distance of 2.77 Å. The hydrogen bond forms between Maltol and the residue proline 565, and the distance of this interaction is measured at 3.28 Å, indicating a weaker hydrogen bond compared to shorter interactions. The oxygen atom of Maltol interacts with GLU91 at a bond distance of 2.12 Å, which signifies a strong interaction. In addition, Maltol's hydrogen atom is involved in hydrogen bonding with GLY82 at a distance of 2.48 Å. Another significant interaction is observed with leucine (LEU)96, where the bond distance is 2.06 Å, indicating a robust molecular interaction. These interactions stabilize Maltol within the binding pocket of HP-5. The 3D and 2D interactions are depicted in Fig. 12.

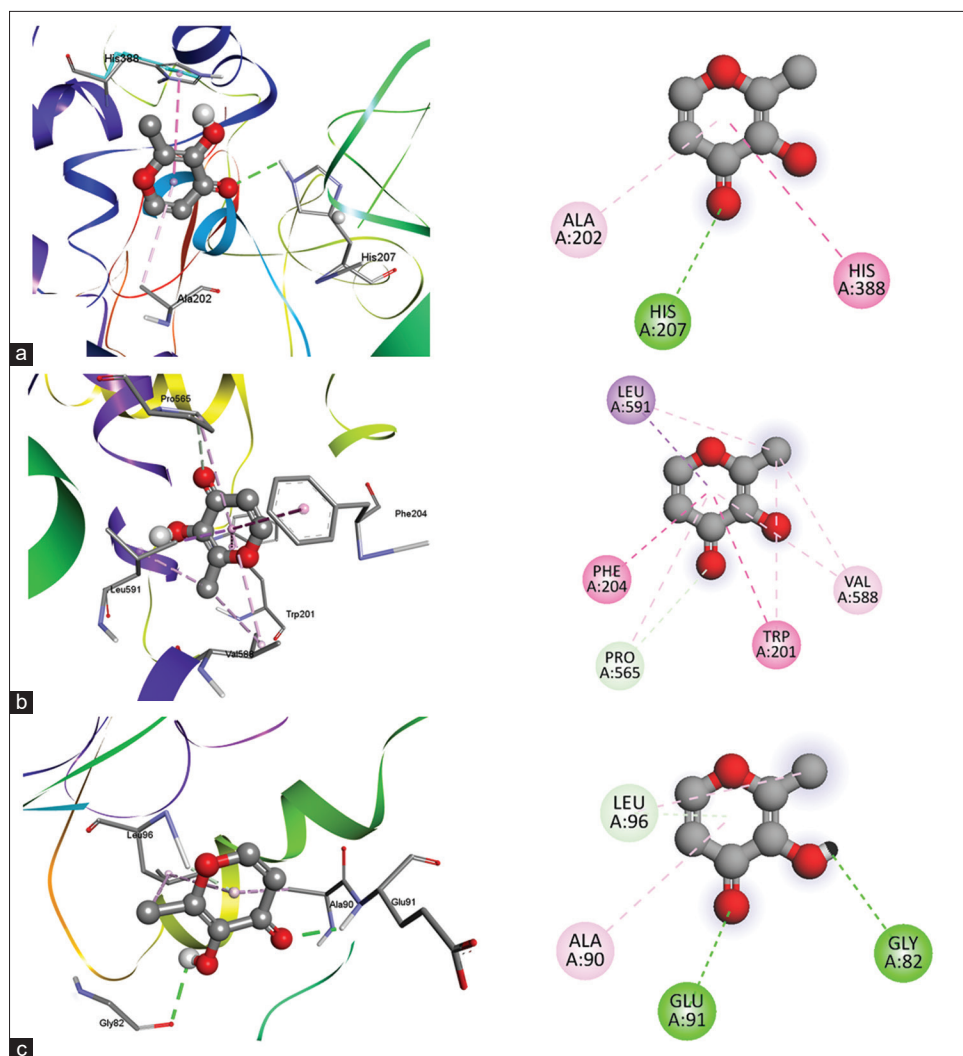


Fig. 12: Molecular interactions and binding affinities of Maltol with (a) cyclooxygenase-2, (b) 5-lipoxygenase, and (c) Human peroxiredoxin 5

The hydroxyl group of 6-Gingerol forms a strong hydrogen bond with the side chain of ARG44 at a distance of 2.05 Å. This interaction is particularly significant due to the positively charged guanidinium group of ARG, which can form stable electrostatic interactions with the oxygen atom of the hydroxyl group. Such an interaction likely plays a key role in stabilizing the binding of 6-Gingerol within the COX-2 active site. In addition, the sulfur-containing side chain of CYS41 forms another hydrogen bond with 6-Gingerol at a distance of 2.42 Å, contributing to the molecule's stabilization within the enzyme. The molecular interaction of 6-Gingerol with the 5-LOX enzyme involves several crucial hydrogen bonding interactions. The side chain of GLN611 is engaged in multiple hydrogen bonds at distances of 2.74 Å, 2.18 Å, and 2.65 Å. The presence of hydrogen bonding between the hydroxyl group of ARG401 at 1.94 Å and the hydroxyl group of 6-Gingerol suggests a strong electrostatic interaction. The distance of 3.30 Å between GLU614 and 6-Gingerol further complements the network of interactions. These interactions likely involve functional groups on the 6-Gingerol molecule such as hydroxyl (OH) and carbonyl (C=O) groups. 6-Gingerol forms a hydrogen bond with HIS160 at a distance of 2.26 Å, indicating a strong interaction. There is a weaker interaction with ASN321 at a distance of 3.57 Å. In the context of 6-Gingerol interacting with HP5, the hydrogen bond is formed between the oxygen atom of the carbonyl group in GLY92 and a hydrogen atom of 6-Gingerol. This interaction occurs at a bond distance of 2.63 Å. In addition, LEU96 participates in another hydrogen bond with 6-Gingerol, where a close interaction is

observed at a bond distance of 1.99 Å. The 3D and 2D interactions are represented in Fig. 13.

The oxygen atom of 2-Amino adipic acid interacts with THR206 at a bond distance of 2.98 Å, another interaction occurs between the oxygen atom and the amino acid HIS207, with a bond distance of 2.54 Å, forming a stable hydrogen bond. The hydrogen bond is formed between the nitrogen atom of 2-Amino adipic acid and tyrosine (TYR)385, with a bond distance of 2.41 Å. These functional groups facilitate the formation of stable hydrogen bonds that anchor 2-Amino adipic acid in the active site, influencing the binding affinity and specificity of the interaction with COX-2. The interactions between the polar functional groups of 2-Amino adipic acid (such as its amino group and carboxyl group) and the amino acid residues of 5-LOX provide a stable network of hydrogen bonds. The amino group (-NH₂) of 2-Amino adipic acid plays a crucial role in forming hydrogen bonds with polar side chains, such as the imidazole ring of HIS624 and the hydroxyl groups of tyrosine residues (TYR81, TYR100, and TYR383). This interaction helps to anchor the ligand in the active site. The carboxyl group (-COOH) of 2-Amino adipic acid can participate in ionic interactions with negatively charged residues, particularly with ASP166. In the molecular interaction between 2-Amino adipic acid and PDE4, the carboxyl group of 2-Amino adipic acid forms hydrogen bonds with key residues such as TYR159 (at 2.35 Å) and HIS160 (at 2.22 Å). In addition, the same functional group interacts with ASP318, forming two hydrogen bonds at distances of 2.33 Å and 2.16 Å, respectively. In the molecular

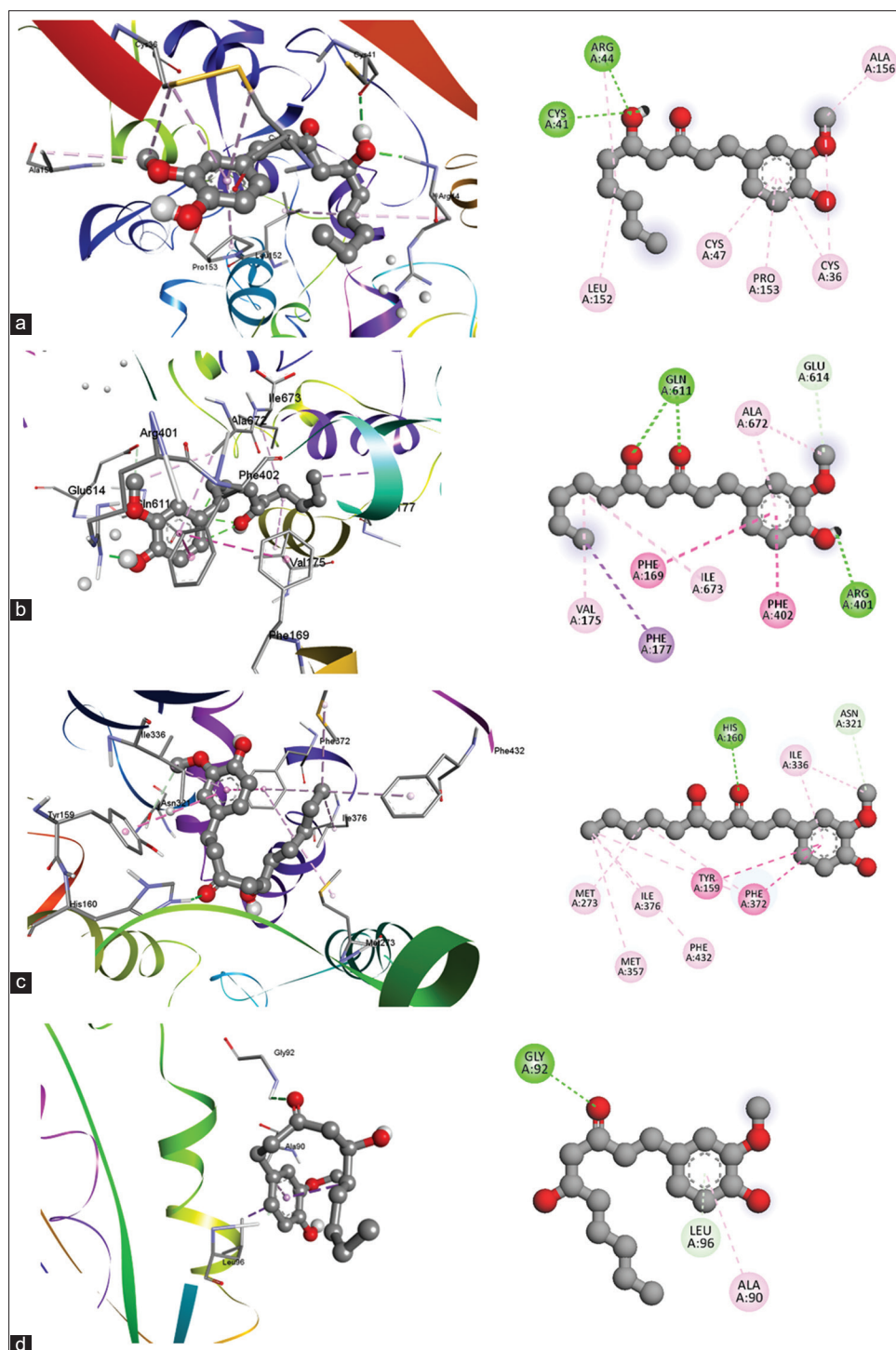


Fig. 13: Molecular interactions and binding affinities of 6-Gingerol with (a) cyclooxygenase-2, (b) 5-lipoxygenase, (c) Phosphodiesterase 4, and (d) Human peroxiredoxin 5

interaction between 2-Aminoadipic acid and HP5, the carboxyl group forms a hydrogen bond with GLY92, with a bond distance of 2.19 Å. In addition, the carbonyl group interacts with VAL70 and lysine (LYS)63, forming hydrogen bonds at distances of 2.65 Å and 3.28 Å, respectively. The interaction with GLN68 and another hydrogen bond with LYS63. The 3D and 2D interactions are represented in Fig. 14.

The results demonstrated that the compounds identified from GC-MS and LC-MS analysis, including Triamcinolone Acetonide, Fluprednisolone,

Maltol, 6-Gingerol, and 2-Aminoadipic acid, previously reported for their anti-inflammatory activity, showed significant binding affinity through both hydrogen and hydrophobic interactions with key targets such as COX-2, 5-LOX, PDE4, and HP5. These strong interactions with crucial inflammatory enzymes highlight their potential as effective anti-inflammatory agents. Further studies targeting other enzymes will provide more insights into the anti-inflammatory properties of *U. distachya*.

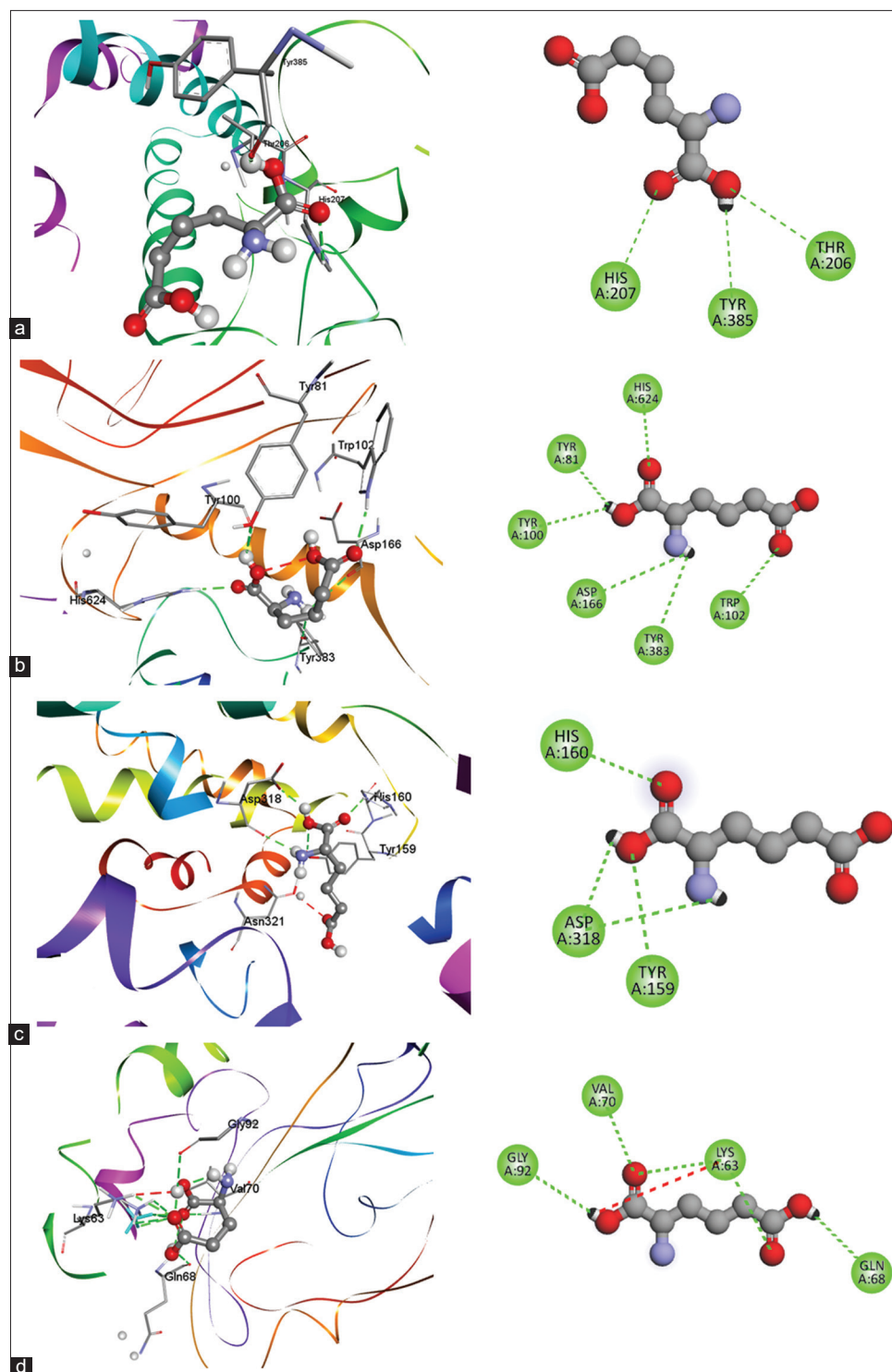


Fig. 14: Molecular interactions and binding affinities of 2-Aminoadipic acid with (a) cyclooxygenase-2, (b) 5-lipoxygenase, (c) Phosphodiesterase 4, and (d) Human peroxiredoxin 5

CONCLUSION

The present study highlights the anti-inflammatory potential of phytoconstituents identified from CUD and EAUD extracts through GC-MS and LC-MS analyses. Both extracts, particularly CUD at a dose of 400 mg/kg body weight, exhibited significant reductions in carrageenan-induced paw edema in rats, with CUD showing more potent activity compared to EAUD. *In silico* molecular docking studies further supported these findings, revealing strong binding affinities

of compounds such as Holothurin acetate, 7, 8-Epoxyanostan-11-ol, 3-acetoxy-, 7,8,12-Tri-O-acetyl-3-desoxy-ingol-3-one, Anodendroside E 2, Triamcinolone Acetonide, Fluprednisolone, Maltol, 6-Gingerol, and 2-Aminoadipic acid with key inflammatory targets including COX-2, 5-LOX, PDE4, and HP5. The binding affinities of these compounds suggest promising anti-inflammatory properties. Further molecular simulations and *in vivo* models are necessary to validate these findings and assess the true therapeutic potential of these compounds. This combined approach could lead to the development of new anti-

inflammatory agents based on the bioactive compounds identified in this study.

CONSENT FOR PUBLICATION

Not applicable.

ETHICS APPROVAL AND CONSENT TO PARTICIPATE

The Animal Ethical Committee (1376/PO/Re/S/10/CPCSEA) approved the study protocol and confirmed the guidelines for animal care and use in scientific research. The project proposal numbers IAEC/01/2024 for the acute toxicity study and IAEC/03/2024 for carrageenan-induced paw edema in rats.

ACKNOWLEDGMENTS

The authors thank the Sophisticated Analytical Instruments Facility (SAIF), IIT Bombay, for assistance with GC-MS analysis; Sophisticated Analytical Instruments Facility (SAIF), IIT Lucknow, for LCMS analysis; and The Pharmaceutical College, Barpali, Odisha, for animal study.

CONFLICTS OF INTEREST

The author declares that they have no conflicts of interest.

FUNDING

No funding was received by the author.

REFERENCES

- Mansouri MT, Hemmati AA, Naghizadeh B, Mard SA, Rezaie A, Ghorbanzadeh B. A study of the mechanisms underlying the anti-inflammatory effect of ellagic acid in carrageenan-induced paw edema in rats. *Indian J Pharmacol*. 2015;47(3):292-8. doi: 10.4103/0253-7613.157127, PMID 26069367
- Medzhitov R. Origin and physiological roles of inflammation. *Nature*. 2008 Jul;454(7203):428-35. doi: 10.1038/nature07201, PMID 18650913
- Gonfa YH, Tessema FB, Bachheti A, Rai N, Tadesse MG, Nasser Singab A, et al. Anti-inflammatory activity of phytochemicals from medicinal plants and their nanoparticles: A review. *Curr Res Biotechnol*. 2023 Jan 1;6:100152. doi: 10.1016/j.crbiot.2023.100152
- Sumathi S, Anuradha R. In-vitro anti-inflammatory activity of flower. *Int J Herb Med*. 2016;4(5):5-8.
- Kabir I, Ansari I. A review on in vivo and in vitro experimental models to investigate the anti-inflammatory activity of herbal extracts. *Asian J Pharm Clin Res*. 2018 Nov 7;11:29-35.
- Eming SA, Krieg T, Davidson JM. Inflammation in wound repair: Molecular and cellular mechanisms. *J Invest Dermatol*. 2007 Mar;127(3):514-25. doi: 10.1038/sj.jid.5700701, PMID 17299434
- Pahwa R, Goyal A, Jialal I. Chronic Inflammation. Treasure Island, FL: StatPearls; 2024.
- Fangkrathok N, Junlatat J, Sripanidkulchai B. In vivo and in vitro anti-inflammatory activity of *Lentinus polychrous* extract. *J Ethnopharmacol*. 2013 Jun 3;147(3):631-7. doi: 10.1016/j.jep.2013.03.055, PMID 23542041
- Sugihartini N, Prabandari R, Yuwono T, Rahmawati DR. The anti-inflammatory activity of essential oil of clove (*Syzygium aromaticum*) in absorption base ointment with addition of oleic acid and propylene glycol as enhancer. *Int J Appl Pharm*. 2019;11(5):106-9.
- Bindu S, Mazumder S, Bandyopadhyay U. Non-steroidal anti-inflammatory drugs (NSAIDs) and organ damage: A current perspective. *Biochem Pharmacol*. 2020 Oct;180:114147. doi: 10.1016/j.bcp.2020.114147, PMID 32653589
- Ghlichloo I, Gerriets V. Nonsteroidal Anti-Inflammatory Drugs (NSAIDs). Treasure Island, FL: StatPearls; 2024.
- Al-Mousawwy J, Al-Hussainy Z, Alaayedi M. Formulation and evaluation of effervescent granules of ibuprofen. *Int J Appl Pharm*. 2019;11(6):66-9. doi: 10.22159/ijap.2019v11i6.34912.
- Nemudzhivadi V, Masoko P. In vitro assessment of cytotoxicity, antioxidant, and anti-inflammatory activities of *Ricinus communis* (Euphorbiaceae) Leaf Extracts. *Evid Based Complement Alternat Med*. 2014;2014(1):625961. doi: 10.1155/2014/625961, PMID 25477994.
- Alfaro RA, Davis DD. Diclofenac. Treasure Island, FL: StatPearls; 2025.
- Lynch S, Brogden RN. Etodolac. A preliminary review of its pharmacodynamic activity and therapeutic use. *Drugs*. 1986 Apr 1;31(4):288-300. doi: 10.2165/00003495-198631040-00002, PMID 2940079
- Lioncino M, Monda E, Palmiero G, Caiazza M, Vetrano E, Rubino M, et al. Cardiovascular involvement in transthyretin cardiac amyloidosis. *Heart Fail Clin*. 2022 Jan 1;18(1):73-87. doi: 10.1016/j.hfc.2021.07.006, PMID 34776085
- Ngo VT, Bajaj T. Ibuprofen. Treasure Island, FL: StatPearls; 2025. Available from: <https://gov/books/NBK542299>
- Indomethacin: Uses, Side Effects, Dosage, Precautions & More. CARE Hospitals. Available from: <https://www.carehospitals.com/medicine-detail/indomethacin>
- Carbone C, Rende P, Comberiat P, Carnovale D, Mammi M, De Sarro G. The safety of ketoprofen in different ages. *J Pharmacol Pharmacother*. 2013 Dec;4 Suppl 1:S99-S103. doi: 10.4103/0976-500X.120967, PMID 24347993
- Meloxicam: Uses, Side Effects, Interactions, Pictures, Warnings & Dosing-WebMD. Available from: <https://www.webmd.com/drugs/2/drug-911/meloxicam-oral/details> [Last accessed on 2025 Jan 18].
- Mefenamic Acid: MedlinePlus Drug Information. Available from: <https://medlineplus.gov/druginfo/meds/a681028.html> [Last accessed on 2025 Jan 18].
- Nabumetone Side Effects, Dosage, Uses, and More; 2017. Healthline. Available from: <https://www.healthline.com/health/drugs/nabumetone-oral-tablet> [Last accessed on 2025 Jan 18].
- Side Effects of Naproxen; 2022. Available from: <https://uk/medicines/naproxen/side-effects-of-naproxen> [Last accessed on 2025 Jan 18].
- Robertson E. Oxaprozin. In: Enna SJ, Bylund DB, editors. *xPharm: The Comprehensive Pharmacology Reference*. New York: Elsevier; 2007. p. 1-7. Available from: <https://www.sciencedirect.com/science/article/pii/B9780080552323623402> [Last accessed on 2025 Jan 18].
- Piroxicam. In: *LiverTox: Clinical and Research Information on Drug-Induced Liver Injury*. Bethesda: National Institute of Diabetes and Digestive and Kidney Diseases; 2012. Available from: <https://www.ncbi.nlm.nih.gov/books/NBK548425> [Last accessed on 2025 Jan 18].
- Sulindac Side Effects, Dosage, Uses, and More; 2017. Healthline. Available from: <https://www.healthline.com/health/drugs/sulindac-oral-tablet> [Last accessed on 2025 Jan 18].
- Cohen B, Preuss CV. Celecoxib. Treasure Island, FL: StatPearls; 2025. Available from: <https://gov/books/NBK535359>
- Rudrapal M, Eltayeb WA, Rakshit G, El-Arabey AA, Khan J, Aldosari SM, et al. Dual synergistic inhibition of COX and LOX by potential chemicals from Indian daily spices investigated through detailed computational studies. *Sci Rep*. 2023 May 27;13(1):8656. doi: 10.1038/s41598-023-35161-0, PMID 37244921
- Rajesh KD, Vasantha S, Panneerselvam A, Valsala Rajesh NV, Jeyathilakan N. Phytochemical analysis, in vitro antioxidant potential and gas chromatography-mass spectrometry studies of *Dicranopteris linearis*. *Asian J Pharm Clin Res*. 2016;9(2):1-6. doi: 10.22159/ajpcr.2016.v9s2.13636
- Shameela KA, Johny J, Ragunathan R. Evaluation of antioxidant, antimicrobial, anticancer, and wound healing properties of leaf extracts of *Acanthus ilicifolius* L. *Int J Curr Pharm Res*. 2023 Jan 15;15:22-9.
- Nunes CD, Barreto Arantes M, Menezes de Faria Pereira S, Leandro da Cruz L, de Souza Passos M, Pereira de Moraes L, et al. Plants as sources of anti-inflammatory agents. *Molecules*. 2020 Aug;25(16):3726. doi: 10.3390/molecules25163726, PMID 32824133
- Patil KR, Mahajan UB, Unger BS, Goyal SN, Belemkar S, Surana SJ, et al. Animal models of inflammation for screening of anti-inflammatory drugs: implications for the discovery and development of phytopharmaceuticals. *Int J Mol Sci*. 2019 Sep 5;20(18):4367. doi: 10.3390/ijms20184367, PMID 31491986
- Bhattacharya A, Tiwari P, Sahu PK, Kumar S. A review of the phytochemical and pharmacological characteristics of *Moringa oleifera*. *J Pharm Bioallied Sci*. 2018 Dec;10(4):181-91. doi: 10.4103/JPBS.JPBS_126_18, PMID 30568375
- Matebie WA, Zhang W, Xie G. Chemical composition and antimicrobial activity of essential oil from *Phytolacca dodecandra* collected in Ethiopia. *Molecules*. 2019 Jan;24(2):342. doi: 10.3390/molecules24020342, PMID 30669366
- Luo L, Gao W, Zhang Y, Liu C, Wang G, Wu H, et al. Integrated phytochemical analysis based on UPLC-MS and network pharmacology approaches to explore the quality control markers for the quality

- assessment of *Trifolium pratense* L. Mol Basel Switz. 2020 Aug 20;25(17):3787.
36. Sasidharan S, Chen Y, Saravanan D, Sundram KM, Yoga Latha L. Extraction, isolation and characterization of bioactive compounds from plants' extracts. Afr J Tradit Complement Altern Med. 2011;8(1):1-10. doi: 10.4314/ajtcam.v8i1.60483, PMID 22238476
 37. El Sayed AM, Basam SM, El-Naggar EB, Marzouk HS, El-Hawary S. LC-MS/MS and GC-MS profiling as well as the antimicrobial effect of leaves of selected *Yucca* species introduced to Egypt. Sci Rep. 2020 Oct 20;10(1):17778. doi: 10.1038/s41598-020-74440-y, PMID 33082381
 38. Baba H, Bunu SJ. Spectroscopic and molecular docking analysis of phytoconstituent isolated from *Solenostemon monostachyus* as potential cyclooxygenase enzymes inhibitor. Int J Chem Res. 2025 Jan 1;9:1-6.
 39. Injeti N, Gubbiyappa KS. GC-MS analysis and in silico approaches of *Indigofera prostrata* and *Lantana camara* constituents for anti-Alzheimer studies. Int J Appl Pharm. 2024 Jul 7;16:100-7. doi: 10.22159/ijap.2024v16i4.50890
 40. Meng XY, Zhang HX, Mezei M, Cui M. Molecular docking: A powerful approach for structure-based drug discovery. Curr Comput Aided Drug Des. 2011 Jun 1;7(2):146-57. doi: 10.2174/157340911795677602, PMID 21534921
 41. Vane JR, Botting RM. Mechanism of action of nonsteroidal anti-inflammatory drugs. Am J Med. 1998 Mar 30;104(3A):2S-8S; discussion 21S-2S. doi: 10.1016/s0002-9343(97)00203-9, PMID 9572314
 42. Funk CD. Prostaglandins and leukotrienes: Advances in eicosanoid biology. Science. 2001 Nov 30;294(5548):1871-5. doi: 10.1126/science.294.5548.1871, PMID 11729303
 43. Torphy TJ. Phosphodiesterase isozymes: molecular targets for novel antiasthma agents. Am J Respir Crit Care Med. 1998;157(2):351-70. doi: 10.1164/ajrccm.157.2.9708012, PMID 9476844
 44. Yang KS, Kang SW, Woo HA, Hwang SC, Chae HZ, Kim K, et al. Inactivation of human peroxiredoxin I during catalysis as the result of the oxidation of the catalytic site cysteine to cysteine-sulfenic acid. J Biol Chem. 2002 Oct 11;277(41):38029-36. doi: 10.1074/jbc.M206626200, PMID 12161445
 45. Cook BG, Pengelly BC, Brown SD, Donnelly JL, Eagles DA, Franco MA, et al. Tropical forages: An Interactive Selection Tool; 2005. Available from: <https://hdl.handle.net/10568/49072> [Last accessed on 2024 Sep 26].
 46. Skerman PJ, Riveros F. Tropical Grasses. France: Food and Agriculture Organization; 1990. p. 900.
 47. Kanupriya KM, Sharma A, Dhiman A. Medicinal potential of *Digitaria*: An overview. J Pharmacogn Phytochem. 2021;10(1):1717-9.
 48. Dash S, Bohidar J, Das C, Mohanty A, Meher A, Hota R. Evaluation of anthelmintic activity and GC-MS characterization of *Urochloa distachya* (L.). Int J Pharm Investigation. 2023;13(2):248-54. doi: 10.5530/ijpi.13.2.034
 49. Dash S, Meher A, Dash SK, Das C, Dash SK. GC-MS analysis of methanolic extract of *Urochloa distachya* (L.) T.Q. Nguyen, leave. Int J Pharm Sci Res. 2022;13(6):2380-94.
 50. Dash S, Bohidar J. GC-MS analysis of methanolic cold extract of *Urochloa distachya* (L.) T.Q. Nguyen, whole plant. Int J Pharm Res Appl. 2021 Sep-Oct;5(6):725-40.
 51. Khandelwal K. Practical Pharmacognosy. Pune: Nirali Prakashan; 2007. p. 7.
 52. Das C, Ghosh G, Rath G, Das D, Kar B, Pradhan D, et al. Chemometric profiling and antiarthritic activity of aerial parts of *Glinus oppositifolius* (L.) Aug. J Ethnopharmacol. 2024 Jun 28;328:117991. doi: 10.1016/j.jep.2024.117991, PMID 38460574
 53. Anonymous. OECD Guideline for Testing of Chemicals. Acute Oral Toxic-Acute Toxic Cl Method; 2001. Guideline 423.
 54. Singh M, Kumar V, Singh I, Gauttam V, Kalia AN. Anti-inflammatory activity of aqueous extract of *Mirabilis jalapa* Linn. leaves. Pharmacogn Res. 2010;2(6):364-7. doi: 10.4103/0974-8490.75456, PMID 21713140
 55. Vecchio AJ, Malkowski MG. The structural basis of endocannabinoid oxygenation by cyclooxygenase-2. J Biol Chem. 2011 Jun 10;286(23):20736-45. doi: 10.1074/jbc.M111.230367, PMID 21489986
 56. Gilbert NC, Gerstmeier J, Schexnaydre EE, Börner F, Garscha U, Neau DB, et al. Structural and mechanistic insights into 5-lipoxygenase inhibition by natural products. Nat Chem Biol. 2020 Jul;16(7):783-90. doi: 10.1038/s41589-020-0544-7, PMID 32393899
 57. Bank RP. RCSB PDB-4WCU: PDE4 Complexed with Inhibitor. Available from: <https://www.rcsb.org/structure/4WCU> [Last accessed on 2024 Oct 01].
 58. Bank RP. RCSB PDB-1HD2: Human Peroxiredoxin 5. Available from: <https://www.rcsb.org/structure/1HD2> [Last accessed on 2024 Oct 01].
 59. Morris GM, Huey R, Lindstrom W, Sanner MF, Belew RK, Goodsell DS, et al. AutoDock4 and AutoDockTools4: Automated docking with selective receptor flexibility. J Comput Chem. 2009 Dec;30(16):2785-91. doi: 10.1002/jcc.21256, PMID 19399780
 60. O'Boyle NM, Banck M, James CA, Morley C, Vandermeersch T, Hutchison GR. Open babel: An open chemical toolbox. J Cheminform. 2011 Oct 7;3(1):33. doi: 10.1186/1758-2946-3-33, PMID 21982300
 61. Dash S, Nanda N, Bhanja M, Sao RB, Roy A, Dash R. GC-MS and molecular docking analyses of phytoconstituents from the plant *Tephrosia purpurea*. J Chem Health Risks. 2024 Sep 10;14(5):196-211.
 62. Hagaggi NS, Abdul-Raouf UM. Production of bioactive β -carotene by the endophytic bacterium *Citricoccus parietis* AUCs with multiple in vitro biological potentials. Microb Cell Factories. 2023 May 3;22(1):90. doi: 10.1186/s12934-023-02108-z, PMID 37138322
 63. Jaber BA, Majeed KR, Hashimi AL. Antioxidant and antibacterial activity of B-carotene pigment extracted from *Parococcus homiensis* strain BKA7 isolated from air of Basra, Iraq. Ann Rom Soc Cell Biol. 2021 May 4;???:14006-28.
 64. Nazir A, Masih M, Iqbal M. Formulation, optimization, qualitative and quantitative analysis of new dosage form of corticosteroid. Future J Pharm Sci. 2021 Oct 16;7(1):208.
 65. El-Rahman GI, Behairy A, Elseddawy NM, Batiha GE, Hozzein WN, Khodeer DM, et al. *Saussurea lappa* ethanolic extract attenuates triamcinolone acetonide-induced pulmonary and splenic tissue damage in rats via modulation of oxidative stress, inflammation, and apoptosis. Antioxidants (Basel). 2020 May;9(5):396. doi: 10.3390/antiox9050396, PMID 32397156
 66. Hoefflich A, Fitzner B, Walz C, Hecker M, Tuchscherer A, Bastian M, et al. Systemic effects by intrathecal administration of triamcinolone acetonide in patients with multiple sclerosis. Front Endocrinol. 2020;11:574. doi: 10.3389/fendo.2020.00574, PMID 32982971
 67. Bakar K, Mohamad H, Tan HS, Latip J. Sterols compositions, antibacterial, and antifouling properties from two Malaysian seaweeds: *Dictyota dichotoma* and *Sargassum granuliferum*. J Appl Pharm Sci. 2019 Oct 4;9(10):47-53.
 68. Godara P, Dulara B, Barwer N, Chaudhary N. Comparative GC-MS analysis of bioactive phytochemicals from different plant parts and callus of *Leptadenia reticulata* wight and arn. Pharmacogn J. 2019;11(1):129-40.
 69. Geetha DH, Rajeswari M, Jayashree I. Chemical profiling of *Elaeocarpus serratus* L. by GC-MS. Asian Pac J Trop Biomed. 2013 Dec;3(12):985-7. doi: 10.1016/S2221-1691(13)60190-2, PMID 24093791
 70. Daffodi ED, Uthayakumar FK, Mohan VR. GC-MS determination of bioactive compounds of *Curculigo orchioides* gaertn. Sci Res Rep. 2012;2(3):198-201.
 71. Hamad D, El-Sayed H, Ahmed W, Sonbol H, Ramadan MA. GC-MS analysis of potentially volatile compounds of *Pleurotus ostreatus* polar extract: In vitro antimicrobial, cytotoxic, immunomodulatory, and antioxidant activities. Front Microbiol. 2022;13:834525. doi: 10.3389/fmicb.2022.834525, PMID 35250951
 72. Zekeya N, Chacha M, Shahada F, Kidukuli A. Analysis of phytochemical composition of *Bersama abyssinica* by gas chromatography-mass spectrometry. J Pharmacogn Phytochem. 2014;3(4):246-52.
 73. El-Sayed ER, Hazaa MA, Shebl MM, Amer MM, Mahmoud SR, Khattab AA. Bioprospecting endophytic fungi for bioactive metabolites and use of irradiation to improve their bioactivities. AMB Express. 2022 Apr 19;12(1):46. doi: 10.1186/s13568-022-01386-x, PMID 35438322
 74. Imad HH, Israa AI, Hawraa JK. Gas chromatography mass spectrum and Fourier-transform infrared spectroscopy analysis of methanolic extract of *Rosmarinus officinalis* leaves. J Pharmacogn Phytother. 2015 Jun 30;7(6):90-106. doi: 10.5897/JPP2015.0348
 75. Al Bratty M, Makeen HA, Alhazmi HA, Syame SM, Abdalla AN, Homeida HE, et al. Phytochemical, cytotoxic, and antimicrobial evaluation of the fruits of miswak plant, *Salvadora persica* L. J Chem. 2020 May 29;2020:1-11.
 76. Laka K, Makgoo L, Mbita Z. Cholesterol-lowering phytochemicals: Targeting the mevalonate pathway for anticancer interventions. Front Genet. 2022;13:841639. doi: 10.3389/fgene.2022.841639, PMID 35391801
 77. Ouimet M, Wang MD, Cadotte N, Ho K, Marcel YL. Epoxycholesterol impairs cholesteryl ester hydrolysis in macrophage foam cells, resulting in decreased cholesterol efflux. Arterioscler Thromb Vasc Biol. 2008 Jun;28(6):1144-50. doi: 10.1161/ATVBAHA.107.157115, PMID

- 18369155
78. Mona MH, Omran NE, Mansoor MA, El-Fakharany ZM. Antischistosomal effect of holothurin extracted from some Egyptian sea cucumbers. *Pharm Biol.* 2012;50(9):1144-50. doi: 10.3109/13880209.2012.661741, PMID 22486556
 79. Arunasalam SB, Karthikeyan N, Thangaiah A, Balasubramaniam R, Thiagarajan A, Jacob R. Active compound analysis of ethanolic extract of roselle calyces (*Hibiscus sabdariffa* L.). *Qual Assur Saf Crops Foods.* 2023;15(2):117-28.
 80. Kushwaha A, Hans N, Giri BS, Rene ER, Rani R. Uncovering the phytochemicals of root exudates and extracts of lead (Pb) tolerant *Chrysopogon zizanioides* (L.) Roberty in response to lead contamination and their effect on the chemotactic behavior of rhizospheric bacteria. *Environ Sci Pollut Res Int.* 2022 Jun;29(29):44998-5012. doi: 10.1007/s11356-022-18887-8, PMID 35146608
 81. Soltan OI, Gazwi HS, Ragab AE, Aljohani AS, El-Ashmawy IM, Batiha GE, et al. Assessment of bioactive phytochemicals and utilization of *Rosa canina* fruit extract as a novel natural antioxidant for mayonnaise. *Molecules.* 2023 Jan;28(8):3350. doi: 10.3390/molecules28083350, PMID 37110582
 82. Alqahtani SS, Makeen HA, Menachery SJ, Moni SS. Documentation of bioactive principles of the flower from *Caralluma retrospiciens* (Ehrenb.) and in vitro antibacterial activity-Part B. *Arab. J Chem.* 2020 Oct 1;13(10):7370-7.
 83. Ahn H, Lee G, Han BC, Lee SH, Lee GS. Maltol, a natural flavor enhancer, inhibits NLRP3 and Non-canonical inflammasome activation. *Antioxidants (Basel).* 2022;11(10):1923. doi: 10.3390/antiox11101923, PMID 36290645
 84. Ziklo N, Bibi M, Salama P. The antimicrobial mode of action of maltol and its synergistic efficacy with selected cationic surfactants. *Cosmetics.* 2021 Sep;8(3):86.
 85. Wang S, Zhang C, Yang G, Yang Y. Biological properties of 6-gingerol: A brief review. *Nat Prod Commun.* 2014 Jul;9(7):1027-30. PMID 25230520
 86. Xiao J, Liu SX, Chen Z, Chiou GC. Vasodilation effects and action mechanisms of TMB-8 on basilar artery in rabbits. *J Cardiovasc Pharmacol Ther.* 1996 Oct 1;1(4):325-32. doi: 10.1177/107424849600100408, PMID 10684433
 87. Bhadoria P, Nagar M, Bharihoke V, Bhadoria AS. Ethephon, an organophosphorous, a fruit and vegetable Ripener: Has potential hepatotoxic effects? *J Fam Med Prim Care.* 2018 May 1;7(1):179-83. doi: 10.4103/jfmpc.jfmpc_422_16, PMID 29915756
 88. Tenny S, Patel R, Thorell W. Mannitol. *StatPearls.* 2024. Available from: <https://www>
 89. Jabłońska-Trypuć A, Pankiewicz W, Czerpak R. Traumatic acid reduces oxidative stress and enhances collagen biosynthesis in cultured human skin fibroblasts. *Lipids.* 2016 Sep 1;51(9):1021-35. doi: 10.1007/s11745-016-4174-5, PMID 27423205
 90. HpODE. BioMol GmbH-life Science Shop; 2024. Available from: [https://www.biomol.com/products/chemicals/lipids/9-hpode-cay10705-50.\(±\)9](https://www.biomol.com/products/chemicals/lipids/9-hpode-cay10705-50.(±)9) [Last accessed on 2024 Aug 28].
 91. Kinyanjui T, Artz WE, Mahungu S. EMULSIFIERS organic emulsifiers. In: Caballero B, editor. *Encyclopedia of Food Science and Nutrition.* 2nd ed. Oxford: Academic Press; 2003. p. 2070-7. Available from: <http://www.sciencedirect.com/science/article/pii/B012227055X004016> [Last accessed on 2024 Aug 28].
 92. Ozturk Sarikaya SB. Acetylcholinesterase inhibitory potential and antioxidant properties of pyrogallol. *J Enzyme Inhib Med Chem.* 2015 Sep 3;30(5):761-6. doi: 10.3109/14756366.2014.965700, PMID 25297710
 93. Oliveira LC, Rodrigues FA, dos Santos Barbosa CR, dos Santos JF, Macêdo NS, de Sousa Silveira Z, et al. Antibacterial activity of the pyrogallol against *Staphylococcus aureus* evaluated by optical image. *Biologics.* 2022 Jun;2(2):139-50. doi: 10.3390/biologics2020011
 94. Kim YI, Hirai S, Takahashi H, Goto T, Ohyan C, Tsugane T, et al. 9-oxo-10(E), 12. *Mol Nutr Food Res.* 2011;55(4):585-93. doi: 10.1002/mnfr.201000264, PMID 21462326
 95. 2-Aminoadipic Acid. *International Journal of Amino Acids.* 2024. Open Access Pub. Available from: <https://openaccesspub.org/international-journal-of-amino-acids/2-aminoadipic-acid>
 96. Methyl 12-Hydroxy Stearate (Methyl-12-HSA) Castor International. 12-hydroxy-Stearate-methyl-12-hsa. Available from: <https://www.castor-international.nl/en/product/methyl>
 97. Saeidian H, Mahdi Mortazavi Asadabad S, Mirjafary Z. Density functional theory studies of maltol derivatives: The effect of heteroatom on aromaticity and antioxidant activity. *Inorg Chem Commun.* 2023 Nov 1;157:111387.
 98. Han NR, Park HJ, Ko SG, Moon PD. Maltol has anti-cancer effects via modulating PD-L1 signaling pathway in B16F10 cells. *Front Pharmacol.* 2023;14:1255586. doi: 10.3389/fphar.2023.1255586, PMID 37731735
 99. Kallay E, Buburuzan L. Vitamin D inflammation and cancer. In: Feldman D, editor. *Vitamin D.* 4th ed., Ch. 102. Academic Press; 2018. p. 891-911. Available from: <https://www.sciencedirect.com/science/article/pii/B9780128099636001024> [Last accessed on 2024 Sep 27].
 100. Basumatary H, Bordoloi P, Deka D. Evaluation of anti-inflammatory activity of aqueous extract of *Mimosa pudica* on swiss albino mouse. *Int J Pharm Pharm Sci.* 2024;16:12-6.